gr-qc 1305.5188

arXiv:1305.5188v1 [gr-qc] 22 May 2013

Gravitational Radiation Detection with Laser Interferometry

Rana X. Adhikari*

Division of Physics, Math, and Astronomy, California Institute of Technology, Pasadena, CA 91125, USA

Gravitational-wave detection has been pursued relentlessly for over 40 years. With the imminent operation of a new generation of laser interferometers, it is expected that detections will become a common occurrence. The research into more ambitious detectors promises to allow the field to move beyond detection and into the realm of precision science using gravitational radiation. In this article, I review the state of the art for the detectors and describe an outlook for the coming decades.

CONTENTS

I. Introduction 1

II. Gravitational Waves 2
A. Response of Interferometer to Space-Time Strain 2
B. Brief Overview of Sources 3
1. Pulsars 3
2. Transients 3
3. Cosmic Background Radiation 4

III. Alternatives to Interferometric Detection 4
A. Acoustic Detectors 4
B. Pulsar Timing 5
C. Artificial Satellite Timing 5

IV. Fundamentals of Interferometric Detectors 5
A. Delay Lines v. Fabry-Perot 5
B. Power Recycling 6
C. Signal Recycling and Extraction 6

V. Sensitivity Limits of Laser Interferometers 6
A. Phase Noise 7
1. Quantum Vacuum Fluctuations 7
2. Scattering from Residual Gas 7
3. Backscatter 7
B. Displacement Noise 8
1. Mirror Thermal Noise 8
2. Suspension Thermal Noise 9
3. Seismic Vibrations 9
4. Newtonian Gravity Noise 10
5. Electromagnetic Coupling 10

VI. First Generation Detectors 11
A. Excess Optical Loss 12
B. Optical Cross-Coupling 12
C. Low Frequency Mirror Motion 14
D. Nonlinear Noise Generation 14
E. Thermal Distortions 15

VII. Second Generation Detectors 15
A. Monolithic Silica Suspensions 16
B. Mirror Metrology 16
C. Dual Recycling 17
D. High Power Opto-Mechanics 18
1. Angular Instabilities 19
2. Parametric Instabilities 20
E. Low Frequency Seismic Isolation 20

VIII. Third Generation Detectors 21
A. Quantum Non-Demolition 21
1. Frequency Dependent Squeezed State Injection 22
2. Frequency Dependent Readout Quadrature 22
3. QND Observable Readout 22
4. Optical Losses and QND 22
B. Circumventing Mirror Thermal Noise 23
1. Non-Gaussian Beam Shapes 23
2. Heteroepitaxial Bragg Mirrors 24
C. Newtonian Gravity Noise Subtraction 24
D. Beyond Silica Suspensions 25
1. Silicon Suspensions 25
2. Electro-Magnetic Suspensions 26

IX. Low Frequency Detectors 26
A. Interferometers in Space 26
1. NGO 26
2. DECIGO and BBO 27
B. Low Frequency Terrestrial Detectors 27
1. Torsion Bar Antenna 27
2. Atom Interferometers 28

X. Conclusion 28

Acknowledgments 28

References 29

I. INTRODUCTION

Nearly a century ago, Einstein predicted the existence of gravitational radiation as a consequence of his General Theory of Relativity (GR) (Einstein, 1916; Einstein, 1918; Einstein and Engel, 1997). For the next several decades, the existence and properties of gravitational radiation were hotly contested within the theoretical community but remained out of observational reach. In 1974, Hulse and Taylor (Taylor *et al.*, 1979) discovered a pulsar in a binary neutron star system. They soon realized that this system serves as an excellent laboratory to test GR. The decrease in the orbital energy of the binary system was found to match the theoretical predictions. During the following decades several other binary pulsars with

* rana@caltech.edu

orbital periods of less than a day have been discovered and the combined data show that the measured energy loss matches exquisitely well with the calculated loss due to the emission of gravitational radiation. Gravitational waves are real.

Modern efforts to detect gravitational radiation on the Earth focus on the use of laser interferometry (Weiss, 1972). Lab scale research throughout the last several decades of the 20$^{\text{th}}$ century lead to the construction of a worldwide network of kilometer scale interferometers (Abbott *et al.*, 2009; Abramovici *et al.*, 1992; Acernese *et al.*, 2008; Lück *et al.*, 2006; Tatsumi, 2008).

Several excellent monographs (Aufmuth and Danzmann, 2005; Barish and Weiss, 1999; Braginsky, 2008; Cella and Giazotto, 2011; Freise and Strain, 2010; Giazotto, 1989; Pitkin *et al.*, 2011; Saulson, 1994; Weiss, 1999) have been written on the techniques of gravitational wave detection by laser interferometry. In this review, we will discuss the current state of gravitational wave detectors, describing in detail the fundamental limits to their astrophysical reach, and then present prospects for the future.

II. GRAVITATIONAL WAVES

In the weak field approximation of General Relativity, the space-time metric, $g_{\mu\nu}$, can be described as (Misner *et al.*, 1973)

$$g_{\mu\nu} \simeq \eta_{\mu\nu} + h_{\mu\nu} \tag{1}$$

where $\eta_{\mu\nu}$ is the Minkowski metric describing flat space and $h_{\mu\nu}$ is the perturbation to the metric due to the gravitational wave. In the transverse-traceless gauge, this can be understood as a *strain* in space-time:

$$h_{\mu\nu}(z,t) = \begin{pmatrix} 0 & 0 & 0 & 0 \\ 0 & -h_+ & h_\times & 0 \\ 0 & h_\times & h_+ & 0 \\ 0 & 0 & 0 & 0 \end{pmatrix} \tag{2}$$

where the two independent polarizations of the wave have amplitudes h_+ and $h_\times$, respectively.

A. Response of Interferometer to Space-Time Strain

In order to relate this perturbed metric with laboratory observables, we can examine how some precision measurement apparatus will respond to such a strain. To illustrate this we can set up two free masses, one located at the origin and one located a distance, $x = L$, from the origin. We can measure the separation between these two masses by sending a laser beam from the origin to bounce off of the far mass and measure the phase of the return beam relative to the source. The accumulated round trip phase is:

$$\Phi_{rt}(t_{rt}) = \int_0^{t_{rt}} 2\pi\nu \, dt \tag{3}$$

where t_{rt} is the time it takes for the light to make one round trip and ν is the frequency of the light. In the absence of radiation, we can do the integral by changing it into an integral over length. To do this we use the flat space metric, $\eta_{\mu\nu}$, to relate space and time for light ($t_{rt} = 2L/c$ and $dt = dx/c$).

In the presence of a gravitational wave, we instead use Eq. 1 to calculate the space-time interval; the perturbed round trip phase is

$$\Phi_{rt}(t_{rt}) = 2\frac{2\pi\nu}{c}\int_0^L \sqrt{|g_{xx}|}\, dx \simeq 2(1 - h_+/2)\frac{2\pi L}{\lambda} \tag{4}$$

in the case of a "plus" oriented wave with a period much longer than the round trip light travel time. Repeating this integral, but doing the integration now along the y-axis, we get that $\Phi_{rt} \simeq 2(1 + h_+/2)(2\pi L/\lambda)$. The difference in the phase shift between the two arms is then $\Delta\Phi \simeq 2h_+(2\pi L/\lambda)$.

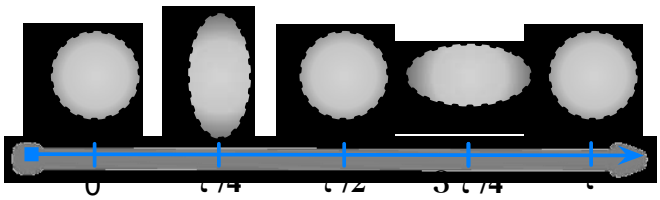

FIG. 1: (Color online)Exaggerated example of the effect of a GW on a ring of test particles. The GW is coming from above, is 'plus' polarized, and has a period, τ. As the wave passes, the ring is alternately stretched and compressed. This quadrupolar strain pattern matches well to the geometry of a Michelson interferometer.

Interpreting the phase shifts as length variations means that the apparent length of each arm is stretched and compressed as the gravitational wave passes. A diagram of this is shown in Fig. 1. The length change is proportional to the original distance between the masses,

$$\frac{\Delta L}{L} = \frac{1}{2}h_+ \tag{5}$$

which is why a gravitational wave is said to cause a strain in space. In contrast, the term 'gravity wave' is usually used to refer to waves in fluids or solids where the restoring force is due to gravity.

The strain along the interferometer arms for a gravitational wave from an arbitrary direction (in spherical coordinates centered on the detector) is:

$$h_{xx} = -\cos\theta \sin 2\phi\ h_\times + (\cos^2\theta\cos\phi^2 - \sin\phi^2)h_+ \quad (6)$$
$$h_{yy} = \cos\theta \sin 2\phi\ h_\times + (\cos\theta^2\sin\phi^2 - \cos\phi^2)h_+ \quad (7)$$

The interferometer response in the low frequency approximation (time scales much longer than the one way light travel time) is proportional to $|h_{yy} - h_{xx}|$. Fig. 2 shows this DC response for + waves, for × waves, and for unpolarized waves (a quadrature sum of the two cases). In the coordinate system used in these plots, the interferometer is located at the origin with the arms parallel to the x and y axes.

B. Brief Overview of Sources

All terrestrial detectors of gravitational waves are focused roughly on the audio frequency band due to technological limits of the detectors and probable source characteristics. In order to verify all of the properties of the waves, one would like to follow in the footsteps of Heinrich Hertz by generating and then detecting the gravitational waves. However, due to the relatively high rigidity of spacetime, it is not feasible to generate measurable amounts of gravitational radiation in the lab (Romero and Dehnen, 1981) by conventional means or even through the use of nuclear explosives arranged to produce quadrupolar mass-energy accelerations (Chapline *et al.*, 1974). Therefore, we look to astrophysical and cosmological sources to provide the radiation. In this way, the hunt for gravitational radiation leads to the development of a new branch of astronomy. Previous overviews (Cutler and Thorne, 2002; Hawking and Israel, 1989) have covered the list of known sources as well as describing the astrophysical and cosmological science that can be extracted from them(Sathyaprakash and Schutz, 2009).

1. Pulsars

One of the earliest predicted sources of gravitational radiation were the recently discovered pulsars (Hewish *et al.*, 1968). The extremely stable period of pulsation of these rotating neutron stars tells us that the energy lost to gravitational radiation must be small (Ipser, 1971) at best. The compensating factor that makes detection a possibility is the periodic nature of the signal; after correcting for the doppler modulations from the detector motions relative to the source (Abbott *et al.*, 2009; Brady *et al.*, 1998), one can improve the signal-to-noise ratio by the square root of the integration time.

Observations (Chakrabarty *et al.*, 2003) of a 'speed limit' for pulsars seem to support the theory (Bildsten, 1998) that gravitational radiation works to brake the spin of the fastest pulsars before they are ripped apart by their relativistic spins. Expectations from neutron star models indicate that the ellipticity may range from $10^{-9} - 10^{-6}$ (Owen, 2006; Ushomirsky *et al.*, 2000) for conventional neutron stars and somewhat larger for more exotic stars (Owen, 2005).

In order to greatly improve the sensitivity of the pulsar searches, the Einstein@Home (Einstein @ Home, 2012) project distributes some of the LIGO data to the home computers of an international team of volunteers. Although no gravitational waves have been detected so far, this project has detected pulsars using electromagnetic astronomical data (Knispel *et al.*, 2011).

2. Transients

The signal which all ground based detectors are aimed towards is the inspiral and merger of compact binary objects: neutron stars (NS) and black holes (BH). Perhaps 1/3 to 1/2 of the stars in the universe have companions (Lada, 2006). Through various mechanisms, some small fraction of these can evolve into a NS/NS, NS/BH, or BH/BH binary (white dwarfs are not quite so compact; mass transfer between the stars begins (Farmer and Phinney, 2003; Lorén-Aguilar *et al.*, 2005) well before the inspiral signal enters the accessible band of the ground based detectors). These compact binaries will eventually merge after they have released their orbital energy through gravitational radiation. The Hulse-Taylor binary is one such binary; it is expected to merge in $\sim 3 \times 10^8$ years. Estimates of the binary merger rates (Belczynski *et al.*, 2002; Phinney, 1991) using bounds from astrophysical observations as well as predictions from population synthesis models vary by a few orders of magnitude. For the upcoming second generation interferometric detectors, the compact binary detection rate may be as low as 1/year or as high as 3/day (Abadie *et al.*, 2010). A combination of extensive analytic methods(Faye *et al.*, 2012) and high accuracy numerical simulations(Ajith *et al.*, 2012; Scheel *et al.*, 2009; Szilágyi *et al.*, 2009) have allowed for the calculation of accurate waveforms by which one can search for these binary inspirals using matched template methods (Allen *et al.*, 2012).

It is most likely that the largest fraction of gravitational wave sources have not yet been modeled well enough to use a template based search. These will include sources such as stellar collapse leading to supernovae (Ott, 2009), the boiling of of the cooling neutron star at the end of the collapse (Liu and Lindblom, 2001), and soft gamma-ray repeaters (Abbott *et al.*, 2008). The most exciting prospect in making a broadband search for gravitational waves is to make a discovery of an entirely unexpected astrophysical phenomenon (Ando

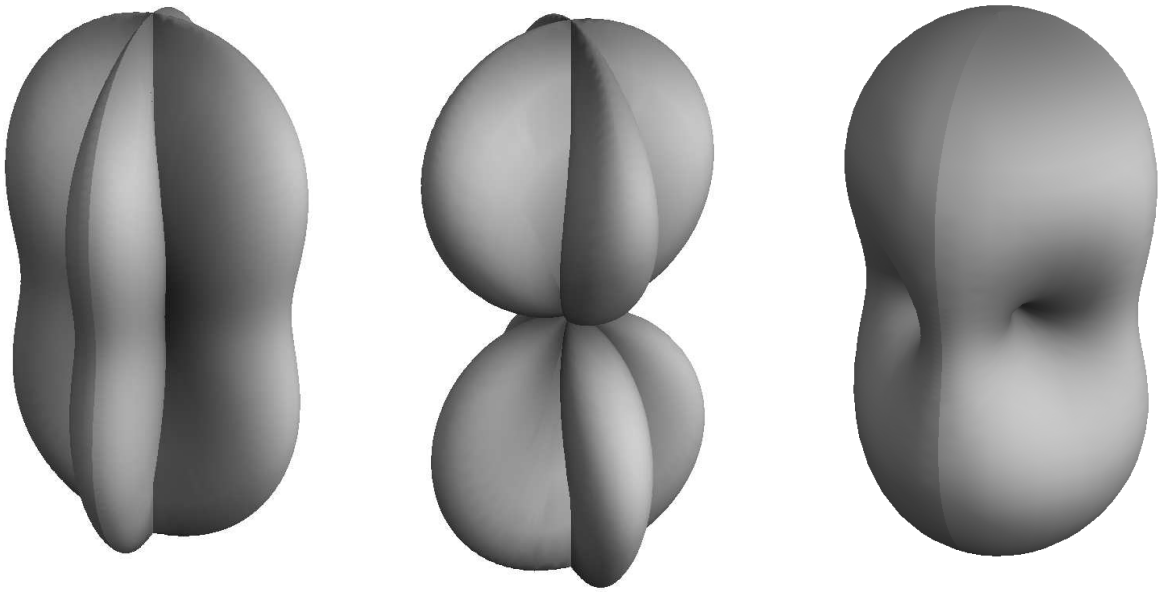

FIG. 2: (Color online) Interferometer Antenna Response for (+) polarization [left], (×) polarization [middle], and unpolarized waves [right]. Color indicates sensitivity (increasing from violet to red).

et al., 2012; Cutler and Thorne, 2002).

3. Cosmic Background Radiation

(Starobinskii, 1979) and others (Abbott and Wise, 1984; Rubakov *et al.*, 1982) pointed our that a period of cosmic expansion in the early universe could produce a spectrum of of gravitational radiation. (Allen, 1988) later derived the full spectrum of gravitational waves expected from a standard inflationary universe scenario. This model predicts a nearly white spectrum (in units of energy) in the frequency band from $10^{-15} - 10^{10}$ Hz(Turner, 1997). This radiation from the early universe would travel to our detectors with very little scattering along the way giving us a direct measurement of the state of the universe less than 10^{-30} s after the Big Bang (Weinberg, 2004). A review of prospects for detecting this inflationary background as well as possible astrophysical foregrounds is given in (Allen, 1997).

There are two observational constraints on the cosmological background of gravitational waves. The relative abundances of the light elements in the universe today constrains tightly any deviations from the standard model in Big Bang Nucleosynthesis (BBN) (Peebles, 1993). An excess of gravitational radiation at the time of BBN would change the expansion rate of the universe. The BBN model places an upper limit of $\sim 10^{-5}$ (in units of the closure density of the universe) on the energy in this primordial gravitational radiation.. Certain exotic theories of the early universe predict higher frequency gravitational radiation(Mandic and Buonanno, 2006; Woodard *et al.*, 2011); for some of those models, a recent search using the LIGO detectors makes a slightly tighter bound (Abbott *et al.*, 2009) than from the BBN model.

III. ALTERNATIVES TO INTERFEROMETRIC DETECTION

A. Acoustic Detectors

Attempts to make a direct detection of gravitational radiation started 50 years ago with Joseph Weber (Weber, 1960, 1970). Weber's claims of detection were never confirmed (Brown *et al.*, 1982; Douglass *et al.*, 1975); a review of these confirmation efforts is given in (Tyson and Giffard, 1978).

Nevertheless, the excitement generated in the early 1970's lead, in the following years, to the development of an active worldwide network of acoustic 'bar' detectors with an ever increasing astrophysical reach. By the end of the 20^{th} century, the bars had reached strain sensitivities of $3 - 7 \times 10^{-19}$ for $\sim$ 1 ms bursts (Ju *et al.*, 2000).

Detector	Location	Freq. (Hz)	Peak Strain (h_c)	Strain Noise (h(f))
ALLEGRO	LSU	900	7×10^{-19}	7×10^{-19}
EXPLORER	CERN	900	7×10^{-19}	7×10^{-19}
NIOBE	UWA	700	5×10^{-19}	7×10^{-19}
NAUTILUS	Frascati	900	6×10^{-19}	7×10^{-19}
AURIGA	Legnaro	900	3×10^{-19}	7×10^{-19}

TABLE I: Best sensitivity of acoustic bar detectors (Ju *et al.*, 2000). Sensitivity is characterized by minimal detectable strain in the bar bandwidth (peak strain) and also the strain noise spectral density at the frequency of best sensitivity.

B. Pulsar Timing

In the late 1970's, Sazhin (Sazhin, 1978) and Detweiler (Detweiler, 1979) pointed out that the regular pulse periods of radio pulsars could be used to search for gravitational radiation in the 10-100 nHz band. For the past three decades, astronomers have used the ever improving timing available for radio antennae and the ever increasing number of known pulsars (Anholm *et al.*, 2009; Hellings and Downs, 1982; Lorimer, 2008; Van Haasteren *et al.*, 2009) to search for a stochastic GW background of cosmological origin as well as the mergers of massive black holes.

C. Artificial Satellite Timing

Doppler tracking of man made spacecraft was proposed as a means of detecting low frequency gravitational waves in 1975 (Estabrook and Wahlquist, 1975). A carrier signal is sent to the spacecraft from the earth, a transponder on the spacecraft sends the signal back, and the frequency of the incoming and outgoing signals are compared. The relative fractional frequency fluctuations, y_2, due to GWs can be written as (Armstrong *et al.*, 2003; Wahlquist, 1987):

$$y_2[t] = -\frac{1-\mu}{2}\bar{\Psi}[t] - \mu\bar{\Psi}[t - \frac{1+\mu}{2}T_2] + \frac{1+\mu}{2}\bar{\Psi}[t - T_2] \quad (8)$$

where μ is the projection of the gravitational wave unit wavevector onto the earth-satellite unit vector, and $\bar{\Psi}$ is a function encoding the response of the satellite signal's response to the two polarizations of gravitational wave. The best sensitivity using this method was achieved (Armstrong *et al.*, 2003) using the 2001-2002 data tracking the Cassini satellite. The strain noise in the 0.01-10 mHz band ranged from $10^{-13} - 10^{-12}/\sqrt{\text{Hz}}$. Prospects for improving this sensitivity have been explored (Armstrong, 2006); improved frequency standards, subtraction of plasma dispersion, and reduction of mechanical vibration in the terrestrial antenna may lead to as much as an order of magnitude improvement. Until a dedicated laser interferometer mission can be launched, satellite tracking will remain the most sensitive probe of gravitational waves in this frequency band (Asmar *et al.*, 2005).

IV. FUNDAMENTALS OF INTERFEROMETRIC DETECTORS

All of the large GW laser interferometers in the past, as well as those planned for the next decade, are essentially Michelson interferometers (as opposed to e.g., Sagnac interferometers (Sun *et al.*, 1996)). As Eq. 4 shows, the measured optical phase shift is proportional to the Michelson arm length; with typical parameters (L ∼1 km, $\lambda \sim 1$ μm, h ∼ 10^{-21}) the phase shift is just 10^{-11} radians. In order to amplify the signal to detectable levels, one would like to increase L by a few orders of magnitude. Unfortunately, the interferometer arm lengths are limited to a few km due to practical constraints (chiefly available land and prohibitively high construction costs). In order to improve the signal-to-noise ratio, the Michelson is enhanced using several compound optical resonators.

A. Delay Lines v. Fabry-Perot

In order to artificially increase the Michelson arm length, one can bounce the light back and forth in the arms to increase the interaction time with the gravitational wave, thereby increasing the optical phase shift. With sufficiently large mirrors, one could construct a Herriott delay line (Beyersdorf *et al.*, 2000; Herriott and Schulte, 1965; Shoemaker *et al.*, 1988) with hundreds of bounces. Drever (Drever, 1983, 1991) proposed to instead use Fabry-Perot optical resonators in place of the delay lines. These cavities have the advantage of combining all of the many 'bounces' of the delay line onto a single spot. This greatly reduces the size, and thereby, the cost, of the mirrors. An added complexity is that the Fabry-Perot cavity must be servo controlled to be within a small fraction of its resonance linewidth in order to operate linearly.

Nearly all of the modern interferometers now use Fabry-Perot cavities instead of delay lines due to issues with scattered light in the latter (Schnupp *et al.*, 1985). The technical servo control issues have been largely solved over the past few decades using multi-degree of freedom extensions (Acernese *et al.*, 2006; Arai and TAMA Collaboration, 2002; Fritschel *et al.*, 2001; Grote, 2003) of the Pound-Drever-Hall RF heterodyne cavity locking technique (Drever *et al.*, 1983)

Fluctuations in the alignment (Acernese *et al.*, 2010a; Grote *et al.*, 2002; Mavalvala *et al.*, 1998; Morrison *et al.*,

1994a,b) and transverse beam size (Mueller *et al.*, 2000) are sensed in a similar fashion.

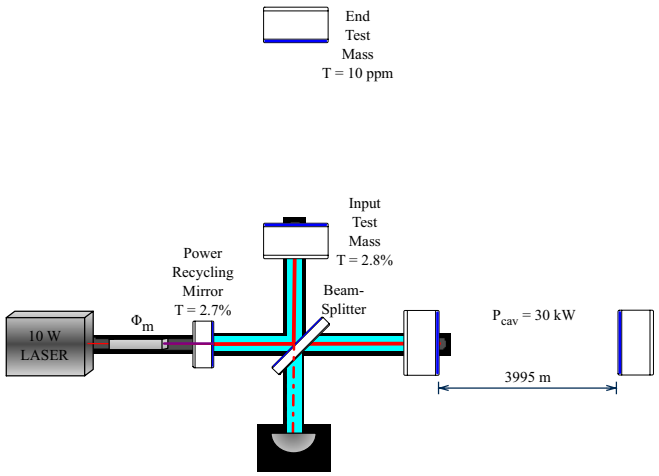

FIG. 3: (Color online) Schematic of the initial LIGO interferometers. The input beam is phase modulated and then build up resonantly in the power recycling cavity. The (cyan) phase modulation sidebands resonate only in the power recycling cavity. The light incident on the photodetector at the bottom of the diagram carries the GW signal.

B. Power Recycling

The interferometer arm cavities are adjusted in length microscopically such that the fields from each arm interfere desctructively at the Michelson anti-symmetric port. This causes almost all of the laser light to return towards the laser. By placing a partially transmitting mirror between the laser and the Michelson beamsplitter, this return light can be made to return towards the beamsplitter interfering constructively with the incoming laser light. The finite transmissivity of this so-called "power recycling (Drever, 1983) mirror" is chosen to nearly equal the total scattering losses from the Michelson's optics and thereby provide optimum power coupling from the laser source into the interferometer arms (GW transducer). In this sense, one can think of the power recycling mirror providing an impedance match to the rest of the interferometer (Fritschel *et al.*, 1992). The modern GW interferometers with Fabry-Perot arm cavities have been able to increase the laser power impinging on the beamsplitter by a factor of ∼65 by using this method. The GEO600 detector has achieved a power gain of 1000 using power recycling (Blair *et al.*, 2012).

C. Signal Recycling and Extraction

Just as a mirror on the symmetric side of the beamsplitter can coherently amplify the power stored in the interferometer, a carefully placed mirror at the anti-symmetric side of the beamsplitter can amplify differential signals (e.g., Fig. 11). This technique is called *Signal Recycling* (Meers, 1988; Mizuno, 1995) and can be used to resonantly build up the GW signal. The GEO600 interferometer (Grote, 2010) has been using signal recycling for the past several years successfully.

The alternative strategy (which is often used in practice) is to use a kind of 'anti-recycling'. To reduce the thermal loading due to bulk absorption in the input test masses, the Fabry-Perot arm cavities are made to have a very high finesse. For the same arm cavity power, this lowers the power level in the optics of the power recycling cavity and allows for a high power to be stored in the cavity with minimal thermal distortions. This narrow linewidth cavity would then normally only amplify the low frequency GW signals (and not the signals above the arm cavity pole frequency) and thereby seem like a nonsensical design choice. However, by adjusting the microscopic position of the 'signal recycling mirror' to form a resonant cavity with the input test mass mirrors, the effective linewidth of the combined system (the differential arm cavity mode + the signal recycling cavity) is broadened. The signal recycling mirror's function has been transformed from signal recycling to resonantly extracting the GW sidebands. This technique is referred to as *Resonant Sideband Extraction* (RSE) (Mizuno *et al.*, 1993; Strain *et al.*, 2003).

These two configurations, signal recycling and resonant sideband extraction, are the extrema of a continuous space of detuning for the signal recycling cavity. The microscopic tuning of this cavity allows for great flexibility in shaping the detector's frequency response (cf. Fig. 12).

V. SENSITIVITY LIMITS OF LASER INTERFEROMETERS

Laser interferometers are limited by two broad classes of noise: displacement noise and phase noise.

Displacement (or *force*) noises work by directly moving the interferometer mirrors. Most of these forces are filtered by the mechanical response of the mirror and its suspension and so are strongly attenuated above several Hz. Many of these force noises can be mitigated by increasing the mass of the mirror.

Phase noises produce fluctuations in the phase of the optical field used to readout the GW strain. These noise sources are only modified by the opto-mechanical response of the interferometer (in nearly the same way as the gravitational-wave strain), and therefore have no strong frequency dependence.

A. Phase Noise

1. Quantum Vacuum Fluctuations

A "fundamental" limit to the sensing of optical phase shifts comes from the stochastic fluctuations in the arrival times of photons at the photodetector. Before 1980, the picture was that a laser interferometer could, at best, be limited by the Poisson statistics. In this picture the signal-to-noise ratio (SNR) for optical sensing would vary as $1/\sqrt{\mathrm{P}}$ (where P is the input laser power) and the fluctuating radiation pressure on the mirror would vary as $\sqrt{\mathrm{P}}$. This description is similar to that of the 'Heisenberg microscope' used to describe uncertainty in introductory physics courses (Feynman, 1965).

A more precise characterization of the quantum measurement limits was derived by Caves (Caves, 1980; Caves and Schumaker, 1985) and others (Loudon, 1981) in the early 1980's. In this picture, the noise arises from the beat between the fluctuations of the vacuum ground state of the electromagnetic field and the stable laser light: vacuum fields entering from the anti-symmetric port split at the beamsplitter, producing differential forces on the arm cavity mirrors (for in-phase fluctuations) and phase fluctuations (for fields which are in the quadrature phase). Vacuum fields at frequencies far from the laser frequency are rejected by the arm cavities, return to the photodetector, and beat with the static field present at the anti-symmetric port (due to both, intentional and unintentional, asymmetries in the arms).

Increasing the laser power leads to a reduction in the measurement uncertainty for the mirror position but increases the amount of momentum perturbations. These momentum perturbations produce position fluctuations after a finite amount of time. Similarly, reducing the laser power reduces the momentum noise but also decreases the positional precision. For a given set of parameters, the laser power may be optimized to give the optimum strain sensitivity at a particular frequency. A detailed analysis of this quantum limit for a free mass leads to the so-called 'Standard Quantum Limit' (SQL) (Braginsky and Khalili, 1999):

$$S_x(f) = \frac{2\hbar}{m(2\pi f)^2} \tag{9}$$

The SQL represents the envelope of minima in the strain noise as the laser power is tuned assuming that the amplitude and phase fluctuations from the vacuum fields are uncorrelated.

At the turn of the century, our understanding of quantum noise in interferometers was revolutionized by the work of Buonanno and Chen (Buonanno and Chen, 2001, 2002) and (Kimble *et al.*, 2001). They showed that the combination of high power and a signal recycling cavity can build up significant quantum correlations within the interferometer. The correlation of the vacuum fluctuations can then allow for significant back action evasion in limited frequency ranges: microscopic detuning of the signal recycling cavity leads to a radiation pressure driven restoring force. This 'optical spring' can be tuned (Miyakawa *et al.*, 2006) via the cavity detuning to optimize the response to different astrophysical sources. Further development of these Quantum Non-Demolition (QND) techniques with application to 3$^{\mathrm{rd}}$ generation detectors is presented in Sec. VIII.A.

2. Scattering from Residual Gas

Fluctuations in the column density of gas in the interferometer arms produce noise in the measured optical phase (Takahashi *et al.*, 2002; Zucker and Whitcomb, 1996). For a single species of molecule, the power spectral density of apparent strain fluctuations is:

$$S_h(f) = \frac{(4\pi\alpha)^2\rho}{v_0 L^2}\int_0^L \frac{exp[-2\pi f\omega(z)/v_0]}{\omega(z)}dz \tag{10}$$

where α is the polarizability, ω is the beam radius, L is the interferometer arm length, ρ is the number density, and v_0 is the most probable speed for the particle. Taking H_2 as an example, it is only necessary to reach a residual pressure of $\sim 10^{-9}$ Torr to reduce the induced strain noise from this molecule to $\sim 10^{-25}/\sqrt{\mathrm{Hz}}$. The partial pressure required for highly polarizable substances, such as hydrocarbons and water, is much more stringent.

3. Backscatter

Imperfections in the mirror shape at spatial scales larger than ∼1 mm (called "figure error"; cf. Fig. 10) can scatter the light incident on the mirrors into small angles that deposit the light into the long beam tubes. Imperfections at smaller spatial scales (called "micro-roughness") will produce a diffuse scatter of the light directly into the nearby vacuum chambers. A small fraction of these scattered light fields is scattered back to the mirror and can then recombine with the circulating field via the mirror imperfections (Flanagan and Thorne, 1995; Thorne, 1989; Vinet *et al.*, 1996; Winkler *et al.*, 1994).

Seismically driven motions of the vacuum system can in this way produce phase and amplitude fluctuations of the light field within the interferometer (Ottaway *et al.*, 2012; Schilling *et al.*, 1981). Works prior to 2012, only included the terms leading to phase modulation of the interferometer's stored field. Since the relative phase between the scatterers and the interferometer field is random, there should be an equal contribution to both the phase and amplitude quadratures. With the increasingly high power levels in modern interferometers, the amplitude component turns out to be *dominant at low frequencies via the influence of radiation pressure* on the

mirror motion. This mechanism is analogous to that of the quantum noise in that the amplitude noise becomes dominant at low frequencies.

Careful engineering of dark, polished, scattered light beam traps throughout the long vacuum tubes and in the vicinity of the mirrors are expected to suppress the influence of the scattered light to below the current quantum backaction limits. Backscatter from the photodetectors used for signal detection can be mitigated by moving the detectors onto a quiet, in-vacuum platform and / or using external phase modulators (Lück *et al.*, 2008).

B. Displacement Noise

All of the following effects produce motion of the test mass through stochastic fluctuation of forces. As such, the power from these types of noise are concentrated at lower frequencies and are not important for higher frequency astrophysical sources (e.g., supernovae, millisecond pulsars, binary neutron star mergers and ringdowns).

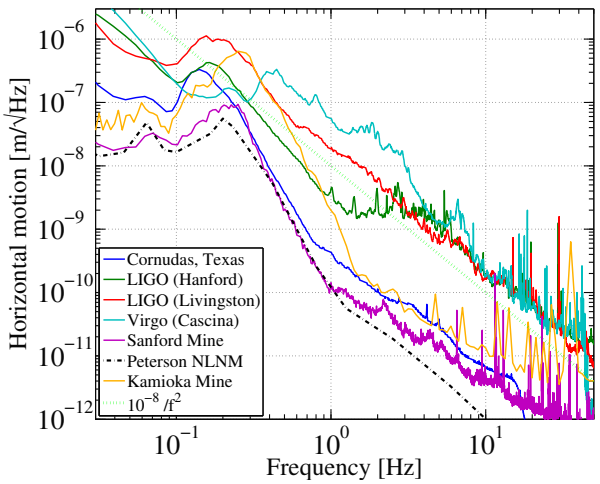

FIG. 4: (Color online). Shown are the seismic vibration spectral density for some of the relatively quiet sites of the current GW detector network. Also shown are two promising locations for future low frequency detectors in the U.S.: the 4100 ft. level of the Sanford Underground Lab and a surface site near El Paso, TX. The USGS New Low Noise Model (Peterson, 1993) is included as a reference. All the spectra here (with the exception of Kamioka (Aso and Araya, 2012)) are estimated using Welch's method but with median instead of mean averaging so as to better reject non-Gaussian transients.

1. Mirror Thermal Noise

When considering fundamental sources of displacement noise for macroscopic objects (such as the interferometer mirrors) we are reminded that the equipartition theorem demands that there be $k_B T$ of energy per mode in any solid which is in thermal equilibrium. In order to determine what the apparent displacement noise fluctuations are for the mirrors, we can compute the spectral density of fluctuations from each mode and then sum them up while including weighting factors for the effective mass in each mode as well as the spatial overlap between the mechanical eigenmode and the laser field distribution (Gillespie and Raab, 1995). This method is quite complicated and converges slowly with increasing mode number.

An alternative approach (González and Saulson, 1994; Levin, 1998), is to directly apply Callen's Fluctuation-Dissipation Theorem (Bernard and Callen, 1959; Callen and Welton, 1951; Kubo, 1966) to the mirror for the laser beam shape in question. Here the power spectrum of apparent displacement fluctuations is:

$$S_x(f) = \frac{k_B T}{\pi^2 f^2} \left| Re\left[Y(f) \right] \right| \tag{11}$$

where T is the temperature of the mirror and $Y(f) \equiv \dot{x}(f)/F(f)$ is the complex mechanical admittance (inverse of impedance) associated with the optical readout beam profile. The meaning of this is the following: in order to determine the level of apparent RMS mirror fluctuation due to thermal forces, we need only to apply a sinusoidal driving force, $F(f)$, and then 'measure' the response. In the case that there is no dissipation, the mechanical response of the system will be entirely in-phase (*modulo* 180 degrees) with the applied force. As with a classical electronic circuit, this orthogonal phase response is proportional to the dissipation: the phase shift between excitation and response is the loss angle (ϕ) or equivalently, $1/Q$ (the Quality factor) of the material.

Following Levin's approach for the mirror thermal noise we can express the displacement noise power spectrum as:

$$S_x(f) = \frac{2 k_B T}{\pi^{3/2} f} \frac{(1-\sigma)}{\omega E} \phi_{sub} \tag{12}$$

where ω is the spot size ($1/e^2$ radius) of the beam, E is the Young's modulus of the mirror substrate, σ is the scalar Poisson's ratio for the substrate, and ϕ_{sub} is the loss angle. The best samples of fused silica, sapphire, and silicon can have loss angles as low as 10^{-8} or better and, as such, do not limit the sensitivity of modern detectors (cf. Fig. 13).

a. Mirror Coating Thermal Noise In fact, the dominant source of thermal noise of the mirror surface is the mechanical dissipation in the dielectric, thin film coating on the mirror surface and *not the bulk mirror material*. These coatings, which have very good optical qualities, are quite poor from the internal friction standpoint. The dependence of this loss on type of material, number of layers, and layer structure have been studied extensively

(Bassiri *et al.*, 2012; Braginsky and Vyatchanin, 2003; Evans *et al.*, 2012; Flaminio *et al.*, 2010; Harry *et al.*, 2007, 2006, 2002; Hong *et al.*, 2012; Kondratiev *et al.*, 2011; Penn *et al.*, 2003; Rowan *et al.*, 2005).

In addition to the Brownian noise, the thermodynamic temperature fluctuations in the coating also produce noise (Braginsky and Vyatchanin, 2003). In this case, however, there is an additional complication: the temperature fluctuations also give rise to fluctuations in the index of refraction of the dielectric thin-films. Since this thermo-refractive noise has the same source as the thermo-elastic noise, they must add (or subtract) coherently (Evans *et al.*, 2008). A judicious choice of the coating layer structure can be used to mostly cancel the effects from these fundamental temperature fluctuations (Harry *et al.*, 2012).

2. Suspension Thermal Noise

A simple example of the power of the Fluctuation-Dissipation theorem for calculating thermal noise is the damped harmonic oscillator (Saulson, 1990). In this case, the admittance is simply

$$Y(f) = \frac{i}{2\pi m} \frac{f}{f_0^2 + i f_0 f/Q - f^2} \tag{13}$$

where f_0 is the resonance frequency of the oscillator. Eq. 13 gives the admittance, and thereby the thermal noise, for an oscillator damped in a *viscous* manner. In the absence of technical limits such as damping from gas in the vicinity of the oscillator (which can be removed through standard vacuum techniques) or friction at the top clamp (Cagnoli *et al.*, 1999; Kovalik and Saulson, 1993) of a pendulum, the mechanical losses in low loss springs and flexures can often be characterized by a constant complex term in the spring constant, $k = k_0(1+i\phi)$, where ϕ, the loss angle is also equal to $1/Q$. This case is often referred to as *structural* damping.

The suspension for the mirrors of the interferometer must serve several purposes: isolate the mirror from ground vibrations, decouple the mirror from the ground to allow it to move freely in response to the gravitational waves, and hold the mirror without introducing extra thermal noise. These needs are simultaneously met by suspending the mirror as a pendulum from a thin fiber.

In contrast to a standard mechanical spring, nearly all of the potential energy for the pendulum is stored in the gravitational field (González and Saulson, 1994; Logan *et al.*, 1993); the pendulum's gravitational spring constant is given by the simple relation: $k_g = mg/l$, where m is the mirror mass, g is the acceleration due to gravity and l is the pendulum length. With this simple model, there would be no damping and the pendulum would have an infinite Q. In reality, there is some energy stored in the bending of the pendulum wire at the two ends. The spring constant for a pendulum supported by N wires is $k_{wire} = N\sqrt{TEI}/2l^2$ (González, 2000; Saulson, 1990), where T is the tension, E is the Young's modulus of the material, and I is the moment of inertia wire's cross section. As this spring is much weaker than the gravitational spring, the overall loss angle of the pendulum can be approximated as $\phi_{pend} = \phi_{wire}(k_{wire}/k_g)$. This reduction factor (the so-called 'dissipation dilution' factor (Cagnoli *et al.*, 2000)) is what allows for having such a low level of thermal noise in a pendulum.

3. Seismic Vibrations

Seismic vibrations of the laboratory prove to be a low frequency limit for all terrestrial laser interferometers. The largest strains of the Earth's surface over km scales are due to the tidal gravity from the Moon and the Sun (Melchior, 1983). These Earth Tides produce length changes of 100-200 microns over a 4 km baseline and for all of the large interferometers are compensated by long-range actuators external to the vacuum system.

In the absence of earthquakes, the next largest component of the ground motion is known as the 'secondary microseism' and occurs at periods of 3-10 seconds (Webb, 1992). This low frequency vibration can sometimes grow to an amplitde of several microns and must be cancelled by an appropriate feedback system. Above ∼1 Hz, the typical vibration spectra for reasonably quiet sites can be approximated as (Aki and Richards, 2009)

$$x_G = 10^{-8} \left(\frac{1\ \text{Hz}}{f}\right)^2 \frac{\text{m}}{\sqrt{\text{Hz}}} \tag{14}$$

To reach astrophysically interesting strain sensitivities ($\sim 10^{-21}/\sqrt{\text{Hz}}$) with a km scale detector therefore requires suppressing the vibrations by a factor of *at least* 10^8 at 10 Hz and 10^6 at 100 Hz.

The best seismic vibration sensors reach a level of $\sim 10^{-13}\ \text{m}/\sqrt{\text{Hz}}$ (Ringler and Hutt, 2010). Incorporating such sensors into active vibration isolation platforms (Hensley *et al.*, 1999; Newell *et al.*, 1997) is useful in reducing the large, low frequency motions and bringing the interferometer close to its useful operating point. The final several orders of magnitude in suppression can only be achieved by using passive isolation. In all of the laser interferometers to date, this passive isolation is roughly the same: a chain of masses and springs isolates the final test mass from the actively controlled platform.

Fig. 5 shows the transfer function from horizontal motion of the ground to motion of the test mass in the laser beam direction. In most cases, this allows one to predict the motion of the test mass given the measurement of the ground noise. This assumption must be corrected for the presence of active vibration isolation systems incorporating seismometers with non-zero internal noise. The

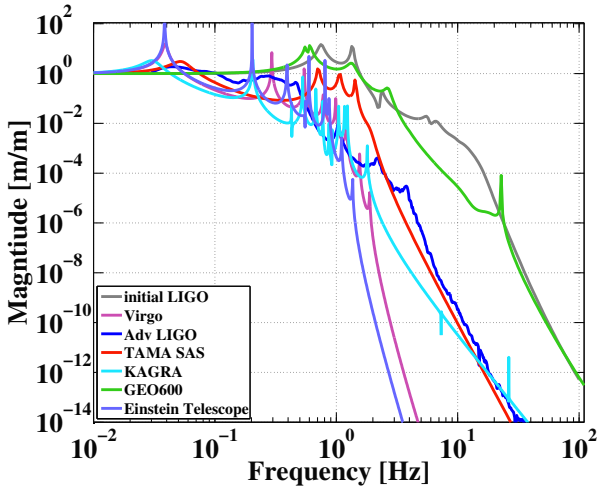

FIG. 5: (Color online). Vibration isolation for the initial LIGO (Giaime *et al.*, 1996; Ponslet and Miller, 1998), Virgo (Accadia *et al.*, 2011a; Acernese *et al.*, 2010b; Ballardin *et al.*, 2001), TAMA (with SAS) (Márka *et al.*, 2002), GEO600 (Grote, 2003; Plissi *et al.*, 1998; Strain, 2012), Adv. LIGO (Abbott *et al.*, 2002), KAGRA(Somiya, 2011), and the Einstein Telescope (Einstein Telescope Science Team, 2011). In the KAGRA case, the mechanical links for cooling (included) are expected to limit the isolation performance above 1 Hz (Takahashi, 2012)

Advanced LIGO isolation system is (intentionally) limited by the noise of these sensors in the 1-10 Hz region and so, instead of a usual transfer function, the ratio of the modeled test mass motion to the ground motion is shown.

A further complication comes from the non-trivial cross-couplings within the isolation systems. Vertical motion and tilts (Giazotto, 2011; Lantz *et al.*, 2009) of the ground couple to the test mass due to mechanical cross coupling in the isolation platforms and mirror suspensions, as well as within the seismic sensors themselves. As such, the transfer functions can only be considered to be approximations of the true vibration isolation levels.

4. Newtonian Gravity Noise

Even with a much improved seismic vibration filtration system, there exists a fundamental limit to terrestrial gravitational experiments (Weiss, 1972). Density fluctuations in the atmosphere and surface waves on the ground can lead to fluctuations in the Newtonian gravitational force (also called gravity gradient noise) on the test masses. Following (Saulson, 1984), this can be approximated as:

$$\delta h_{NN}(f) = \frac{G}{\sqrt{3}\pi}\frac{\rho_E}{L}\frac{x_{GND}(f)}{f^2} \qquad (15)$$

where G is the gravitational constant, ρ_E is the density of the nearby ground, L is the interferometer arm length, and x_{GND} is the ambient ground noise. More sophisticated treatments of the correlations among the seismic waves (Beccaria *et al.*, 1998a; Hughes and Thorne, 1998), atmospheric perturbations (Creighton, 2008) and anthropogenic influences (Thorne and Winstein, 1999) concluded that these Newtonian gravity fluctuations would nearly limit the performance of the 2nd generation detectors in the 5-15 Hz band.

A detailed survey of the sources of vibration at the LIGO sites (Driggers and Harms, 2011) has taken into account vibrating machinery, ambient acoustics, and resonances of the surrounding structures in the laboratory; the resulting estimate is shown in Fig. 6. Although the seismic and acoustic sources which produce these forces can themselves be filtered out, there is no way to shield the test masses from their gravitational forces. It is likely that the Newtonian noise will exceed the quantum back-action limits at low frequencies (see Fig. 13). Mitigation strategies are discussed below in Section VIII.C.

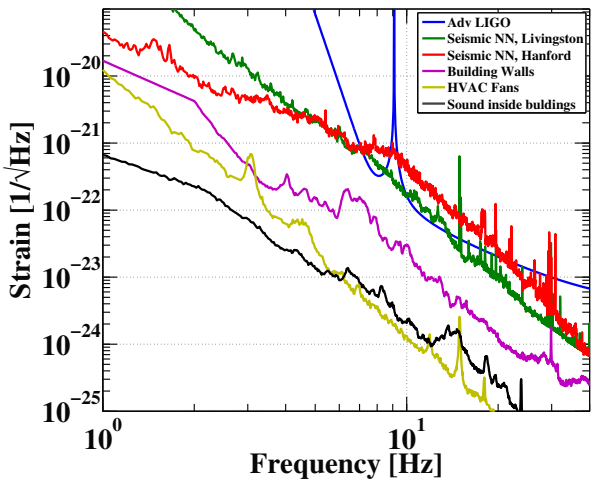

FIG. 6: (Color online). Estimate of the Newtonian gravity noise at the LIGO sites compared to the fundamental thermodynamic and quantum limits for Advanced LIGO. The dominant contribution is from surface waves on the nearby ground. Vibrations of the building walls and acoustics within the building are not very significant. The turbulence from wind outside of the building primarily couples through the vibration of the building walls and is therefore already included in this estimate.

5. Electromagnetic Coupling

In addition to the forces mentioned above, the mirrors of the interferometer may be disturbed by spurious electromagnetic forces: ambient fluctuations of the local electric and magnetic fields, as well as impacts from the background of cosmic rays.

Detector	TAMA	GEO	Virgo	LIGO 2 km	LIGO 4 km
Arm Length [m]	300	600	3000	2009	3995
Mirror Mass [kg]	1	5.5	21	10.5	10.5
Beam Spot Size [cm]	0.85	2.4	2.1	3.5	3.5
# of seismic stages	0 + 1 + 4	1 + 3 + 3	0 + 1 + 6	1 + 4 + 1	1 + 4 + 1
Stored Power [kW]	1	5	20	30	50
Strain Noise $[10^{-23}/\sqrt{\text{Hz}}]$	150	20	6	5	2
Sensitive Band [kHz]	0.3 - 10	0.3 - 5	0.02 - 3	0.06 - 2	0.06 - 2
Location	Japan	Germany	Italy	USA	USA

TABLE II: Comparison of first generation interferometers. The numbers in the '# of seismic' row refer to the number of external active, internal passive, and pendulum suspension stages, respectively. For TAMA and LIGO, substantial hardware upgrades to the seismic isolation took place during the commissioning phase - these numbers refer to the post upgrade configurations.

a. Cosmic Rays At sea level, the stationary background of high-energy cosmic rays is dominated by muons. Within the typical mirror volume of $\sim$0.02 m^2, there are $\sim 10-50$ muons passing through per second (Braginsky *et al.*, 2006; Weiss, 1972). The muons deposit energy in the mirrors by exciting (or ionizing) the electrons bound by the molecules in the material. The Bethe formula (Poenaru and Greiner, 1997) tells us that most of the particles pass through the mirror depositing $\sim$100 MeV in kinetic energy. The false alarm rate (rate of apparent GW signals) due to these high energy muons is extremely low; they can practically be rejected by demanding a coincidence between remote interferometers for making gravitational wave detections. The background of low energy muons, however, leads to a stationary noise spectrum given by (Yamamoto *et al.*, 2008):

$$h_{cosmic}(f) \simeq \left[10^{-27} - 10^{-26}\right] \frac{100 \text{ Hz}}{f} \qquad (16)$$

with some variation between fused silica, sapphire, and silicon (the most common mirror materials for GW detectors). This noise source is 2-3 orders of magnitude lower than the standard quantum limit for all of the present, and envisaged future detectors.

b. Ambient Magnetic Fields The ambient magnetic field fluctuation spectra are fairly broad. As measured at several sites in the U.S. they show a characteristic $1/f$ behavior (Campbell, 1965); at the LIGO sites this $1/f$ character has been observed with an amplitude of $B(f) \sim (10^{-11}/f)$ T$/\sqrt{\text{Hz}}$. In nearly all laboratories on the earth, the dominant features in the spectrum are the harmonics of the AC power line (60 Hz in the U.S.; 50 Hz at the GW detector sites in Italy, Japan, and Germany). At lower frequencies (5 - 50 Hz), the dominant magnetic field fluctuations in the horizontal direction are due to the Schumann resonances (ELF traveling waves within the Earth's surface-ionosphere cavity) and appear as a broad set of peaks at multiples of $\sim$7 Hz (Balser and Wagner, 1960; Volland, 1995). The amplitude of these peaks changes diurnally and also with the intensity of distant lightning activity.

These magnetic fluctuations couple in to the interferometer chiefly through the magnets which are used to actuate the interferometer's mirrors. In the 2$^{\text{nd}}$ generation GEO and LIGO detectors, the magnets have been removed from the test mass mirrors. The magnets on the next closest mirror in the suspension chain may also provide too strong of a coupling path depending upon the magnitude of local ferromagnetic components (which cause gradients).

c. Surface Charge Surface charges on the arm cavity mirrors can produce spurious forces on the mirrors through interaction with nearby conducting surfaces (e.g., the mirror suspension frames) (Mitrofanov *et al.*, 2004; Pollack *et al.*, 2010; Ugolini *et al.*, 2008). These charges may build up through the friction induced by the movements of dust during the evacuation of the chambers. Random fluctuations of the charges could produce force fluctuations comparable to the thermal and quantum limits for the mirror, however, current estimates and measurements are not yet accurate enough to make the case. To be safe, several mitigation strategies are being pursued, including irradiation of the mirror surface with UV light (Sun *et al.*, 2006) and occasionally introducing small amounts of an ultra pure ionized gas into the vacuum chambers.

VI. FIRST GENERATION DETECTORS

The first generation of long baseline interferometers formed the first broadband worldwide network for gravitational wave detection. The network was comprised of TAMA (300 m) near Tokyo, Japan (Arai *et al.*, 2009; Takahashi *et al.*, 2008); GEO (600 m) near Hannover, Germany (Grote, 2003, 2010); Virgo (3 km) near Pisa, Italy (Accadia *et al.*, 2012; Barsotti, 2006); and the LIGO

interferometers (Abbott *et al.*, 2004a, 2009; Abramovici *et al.*, 1992; Adhikari, 2004; Fricke *et al.*, 2012) - a 4 km one in Livingston, LA and in Hanford, WA both a 2 km and a 4 km interferometer in the same vacuum system. Table II lists some of the key parameters of these detectors.

The installation and initial commissioning of these detectors started in the late 1990's. Although more advanced techniques were known at the time, these first generation instruments were built with some conservatism and therefore had several similarities. TAMA300, Virgo, and the three LIGO detectors were configured as power-recycled, Fabry-Perot Michelson interferometers. The GEO600 interferometer was the least conservative of all and included three 'Advanced' techniques: dual-recycling, triple suspensions, and fused silica fibers to hold the mirrors.

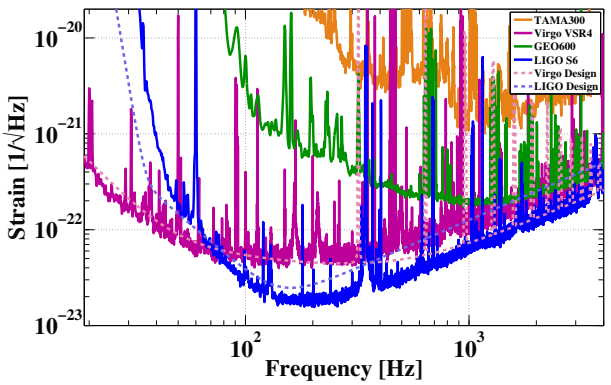

FIG. 7: (Color online). Strain noise for the first generation detectors. TAMA300, GEO600, Virgo+, and Enhanced LIGO. Also shown (dashed) are the strain noise goals for the initial Virgo and LIGO detectors.

The reasonably good agreement between the initial design sensitivity goals and the final performance of the LIGO and Virgo detectors may lead to a false confidence in the accuracy of those early estimates. In reality, the commissioning period for all of the initial interferometers extended over several years and greatly enhanced the understanding of the large interferometers. In all cases, major hardware changes were made in order to bridge the gap between the early performance and the science goals.

In the TAMA interferometer, the initial seismic isolation was replaced with a more elaborate (Virgo-like) system to greatly reduce the seismic noise in the 1-100 Hz band (Takahashi *et al.*, 2008). For the GEO600 detector, an active seismic feedforward system, a thermal compensation system, and scattered light mitigation techniques have been installed over the years. The Virgo interferometer was upgraded with an active thermal lens correction system, isolation optics between the laser and the interferometer (Collaboration, 2008; Collaboration, 2010), as well as numerous control system upgrades (Accadia *et al.*, 2010a; Accadia *et al.*, 2011). LIGO also added a thermal compensation system, as well as an active seismic isolation system for the Louisiana interferometer (Abbott *et al.*, 2004b; Hardham *et al.*, 2004), acoustic isolation chambers for the external optics, and an extensive upgrade to the digital control system.

Between the operation of the initial detectors and installation of the second generation detectors, there was an additional scientific data taking run which followed major hardware upgrades of the Virgo and LIGO detectors (Virgo+ and Enhanced LIGO) which incorporated several of the technologies in development for the second generation machines.

In the rest of this Section, the most significant unexpected or non-ideal features are described as well as the associated mitigation strategies.

A. Excess Optical Loss

With the use of power recycling, nearly all of the laser light is coupled into the interferometer. Good matching between the interferometer arms ensures that only a small fraction (∼few percent) escapes out of the anti-symmetric port. Most of the laser power entering the interferometer is scattered into the surrounding vacuum system. For all of the interferometers, the measured optical losses were significantly higher than expected from the initial, table-top measurements (Sato *et al.*, 1999). A small fraction of the losses came from absorption in the mirror substrate and on the high reflectivity dielectric mirror coatings within the Fabry-Perot arms (in the case of LIGO, Virgo, and TAMA) (Brooks *et al.*, 2009; Hild *et al.*, 2006; Ottaway *et al.*, 2006). Depending upon the level of contamination, the absorption of the mirror surfaces ranged from 1-10 ppm, leading to a wide range of problematic thermal gradients in the mirrors.

d. Scatter Losses As described below (Sec. VII.B), perturbations in the mirror surface can scatter light out of the interferometer. This scatter loss is the chief limit to the power buildup within the resonant cavities. Although ∼ppm level losses have been observed in small optical cavities (Rempe *et al.*, 1992; Uehara *et al.*, 1995), the round trip losses in the Fabry-Perot arms of these large interferometers ranged from 100 ppm (LIGO) to 300 ppm (Virgo)(Acernese *et al.*, 2007). A small fraction of this was due to point defects (cf. Fig. 10) in the mirror coating. The largest fraction of the loss was due to ∼few cm scale perturbations of the mirror surface.

B. Optical Cross-Coupling

All of the interferometers have been designed with a high level of symmetry to passively reject many noise

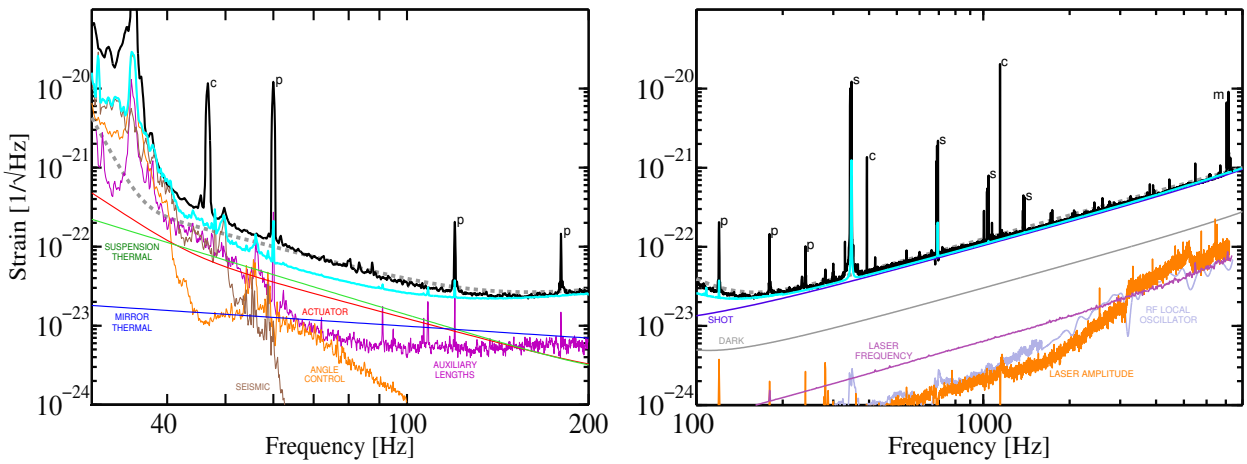

FIG. 8: (Color online)Noise Budget of the LIGO Hanford 4 km detector during the fifth LIGO science run (S5)(Abbott *et al.*, 2009). The plot on the left shows mainly the noise sources which act as a force on the mirrors. The plot on the right shows noise sources which appear as a phase noise on the light. The known peaks in the measured strain data are indicated as (p) for power lines, (c) for calibration lines, (s) for the violin modes of the mirror suspension, and (m) for the mirror's internal eigenmodes. The CYAN trace is a quadrature sum of all known noise sources and the BLACK trace is the measured strain output of the interferometer. The discrepancy between the CYAN and BLACK traces remains unexplained but is suspected to be due to excess friction in the suspension wire attachments to the mirror. The dashed trace is the initial LIGO Science goal.

sources. Differential phase shifts in the interferometer arms (e.g., strain from a gravitational wave) directly produce a signal at the anti-symmetric port. Fluctuations of the incoming laser light or motions of the other mirrors also coupled through to the GW channel in (sometimes) unexpected ways and new techniques were developed to combat these issues.

e. Fluctuations of the Light The Michelson topology, in particular, is largely insensitive to amplitude and frequency fluctuations of the illuminating laser light. By adjusting the length of the interferometer arms microscopically, the anti-symmetric port is made to be nearly dark. In this 'dark fringe' condition the common mode rejection ratio for laser frequency noise was found to be ∼200-1000 for the various interferometers, limited by the imbalance in scatter losses between the arms. Laser power fluctuations can directly drive the mirrors through radiation pressure and in imbalance in the power in the arms. Power fluctuations can also produce apparent mirror fluctuations due to gain modulation of quasi-static offsets in the length control feedback loops of the interferometer. Some of these operating point fluctuations are driven by seismic motion and so this noise source comes from the *product* of seismic motion and laser power fluctuations.

f. Local Oscillator Phase Noise In the TAMA, LIGO, and Virgo interferometers, the scheme which was used to read out differential arm cavity strain is similar, mathematically, to the standard Pound-Drever-Hall technique which is widely used with simple, rigid cavities. An important difference, however, is that both the carrier field and the RF sidebands travel through a few optical cavities before being optically recombined on the anti-symmetric port photodetector (cf. Fig. 3).

In principle, phase noise of the oscillator used to generate the RF sidebands would cancel during the demodulation of the heterodyne signal. The electronic local oscillator used in the demodulation, however, is not filtered by these optical cavities. Furthermore, the filtering experienced by the optical sideband fields is not as simple as might be envisaged by modeling the process by propagation of plane waves (Camp *et al.*, 2000). Each of the higher order transverse modes of the sideband field experiences a different phase shift in the cavities (Ballmer, 2006; Grote, 2008). In this way, the final recombined signal depends in a detailed way on the mirror surface perturbations, and as explained below in Sec. VI.E, on the thermal state of the recycling cavity optics.

In order to reduce this noise to below the shot noise limits, multiple strategies were employed: the mirror curvatures were adjusted with auxiliary heating lasers, the cavity lengths were microscopically adjusted to match the optical and electronic paths, and finally, an ultra low noise crystal oscillator (Wenzel, 2012) was used to reduce the source term by an order of magnitude (to a phase noise level of $< -160\,\mathrm{dBc/Hz}$).

g. Motion of Auxiliary Mirrors Longitudinal motions of the other mirrors in the interferometer (i.e. the power recycling mirror and the beamsplitter) couple to the GW readout weakly (Regehr, 1995), but not so weakly that they can be completely neglected.

Motion of the beamsplitter (or more precisely, differential motion of the short Michelson interferometer formed by the beamsplitter and the input test masses) couples in the usual way; the mirror motion modulates the phase of the carrier field and produces a signal as if it was a gravitational-wave. This produces a weaker signal since it does not experience the resonant build up of the arm cavities. However, this mirror has noise imposed on it by its feedback control loop which is orders of magnitude above the shot noise limits of the GW channel. In order to recover the quantum limited performance of the interferometer, this feedback noise was filtered and injected into the end mirrors so as to cancel the initial noise injection (Fritschel *et al.*, 2001). This *feedforward* path was able to cancel the noise by a factor of $\sim 30-100$ (for LIGO) in the most sensitive frequency band. The Virgo feedforward system achieved several times more cancellation by using an adaptive gain in this path (Acernese *et al.*, 2010).

The coupling of the power recycling mirror motion is less straightforward. This motion only produces a signal through the existence of asymmetries. The imbalance in the amplitude reflectivity of the arm cavities produces a carrier field at the anti-symmetric port which is in the orthogonal phase from the gravitational wave signal sidebands. The power recycling mirror motion modulates the phase of the RF sidebands and couples this orthogonal phase field into the GW channel. This coupling was $\sim 10\times$ smaller than the Michelson coupling, but was dealt with in essentially the same way, although the achieved cancellation factor was several times smaller.

Removing these noise sources allowed the interferometers to operate much closer to their fundamental limits. An unpleasant side-effect is that the residual noise from these processes is highly non-stationary, almost by definition. The static coupling path is cancelled by these electronic cancellation paths, but time variation in the opto-mechanical properties of the interferometers (due to temperature, seismic noise, beam pointing, optical losses, etc.) produces large fluctuations in the residual coupling. The next generation interferometers have the added complexity of also needing to cancel the motion of the signal recyclng cavity, but the added benefit of having much less low frequency mirror motion resulting in less variation in the coupling constants.

C. Low Frequency Mirror Motion

Simple estimates of the coupling of seismic vibration (e.g., Sec V.B.3) to the interferometer's strain channel assume that the coupling is essentially linear. During the decade spent commissioning these interferometers, it became clear that this assumption fails in a myriad of ways: large, low frequency motion produces noise in the GW detection band.

h. Seismic Amplification As can be seen from Fig. 5, below 1 Hz, many of the isolation systems amplify the ground noise. In the case of the passive systems this comes from the lowest natural frequencies of the stacks and suspensions. In the case of the active systems, this can come from the coupling of tilts into the active sensors or insufficient phase margin in the control systems. These low frequency peaks are necessary to have steep attenuation at higher frequencies. Unfortunately, this design tradeoff leads to an amplification of motion in the anthropogenic band which can be highly non-stationary(Accadia *et al.*, 2011b; Acernese *et al.*, 2004; Daw *et al.*, 2004; Saccorotti *et al.*, 2011).

i. Noise from Damping In order to mitigate this problem, the suspension systems were designed to have some capability of using 'cold damping': sensors local to each test mass can be used to sense and suppress these high amplitude, low frequency motions. This is only partially successful. Although it is possible to reduce the motion somewhat, it proved impossible to completely compensate the amplification without introducing excess noise into the GW signal band. The feedback filters must obey the Kramers-Kronig relations.

For the interferometer mirrors in the recycling cavity / Michelson area, the situation is more complicated. Optics which are separated by much less than a seismic wavelength move coherently. In the absence of active feedback systems, the differential motion among these optics is highly suppressed. The noise of the local damping sensors has no such correlation, however. Attempting to apply damping in such a situation actually amplifies the relative interferometric length fluctuations at low frequencies. In practice, these issues require the delicate tailoring of the local damping feedback filters and limits how strong the damping of the high Q mechanical resonances can be.

D. Nonlinear Noise Generation

These large, low frequency motions all conspire to produce noise in the GW band through several different nonlinear mechanisms.

j. Bilinear Angle to Length Conversion The large ground motions in the 0.1-1 Hz band produce angular fluc-

tuations in the interferometer mirrors through cross-couplings in the vibration isolation and suspension systems; the source of the angular motion is chiefly horizontal motion of the ground and not tilt. These fluctuations are partially cancelled by a complicated control system (Acernese *et al.*, 2006; Grote *et al.*, 2002; Mavalvala *et al.*, 1998) based on RF heterodyne detection of the optical wavefronts on quadrant photodetectors and feedback through a MIMO (multiple input - multiple output) digital signal processing system. The control system feeds some of the sensor noise in the GW detection band back into the mirrors. The mirror actuators are balanced so as to place the axes of rotation of the mirror at the center of the laser beam spot position and this cancels the coupling of angular noise to interferometer strain readout, to first order (Tatsumi *et al.*, 2006). Due to the residual low frequency mirror motions, the resonating laser beam moves around with respect to this null point by hundreds of microns. The angle to strain coupling is therefore, nonstationary (Dooley, 2011). During intense storms or times of high anthropogenic seismicity, the low frequency noise of the detectors would become compromised by this nonstationary noise source.

k. Actuator Nonlinearities In order to maintain the resonance condition of the interferometer, the control system must compensate for the ∼micron scale motions below 1 Hz while simultaneously introducing less than 10^{-19} m of motion in the GW band around 100 Hz. This requires the mirror actuator to be highly linear: the upconversion of force noise must be less than 1 part in 10^9. While such a high dynamic range is just possible with modern low noise electronics, it is not feasible to do so using magnetic actuators, due to the Barkhausen effect(Barkhausen, 1919; Bertotti, 1998; Bittel, 1969; Durin and Zapperi, 2004). The low frequency control forces are applied to the mirror using magnet-coil pairs. The time-varying control forces, which are used to compensate for the seismic motions, induce domain flips in the more loosely bound domains of the magnets attached to the mirrors. In the NdFeB magnets used in LIGO and TAMA, there were many weakly bound domains and the Barkhausen effect exhibited a force noise upconversion of 1 part in 10^7. The Virgo interferometer was instrumented with SmCo magnets which have a much smaller Barkhausen effect. However, any nearby ferromagnetic materials can lead to this fluctuating magnetic noise (Schofield, 2010). Future interferometers are being designed to use multiple chain pendulums (as in Virgo and GEO) so as to minimize the dynamic range requirements. To minimize the magnetic coupling, either the magnets will be down-sized drastically or eliminated altogether in favor of electrostatic actuators.

E. Thermal Distortions

The small, but non-zero, optical absorption in the mirrors of the interferometers produced significant thermal gradients within the optics. These gradients produced distortions of the mirror surface (thermal expansion of the glass) as well as a significant thermal lensing within the substrate (temperature dependence of the refractive index) (Hello and Vinet, 1990, 1993; Strain *et al.*, 1994; Winkler *et al.*, 1991). The presence of low levels of contaminants on the optics' surfaces lead to higher than anticipated levels of absorption.

There are several mechanisms by which thermal distortions can lead to instability and degraded noise performance in the interferometers. The simplest mechanism is through reduction of signal; differential thermal lensing in the input test mass mirrors reduces the spatial overlap of the GW signal sidebands with each other. This contrast defect also increases the shot noise level at the anti-symmetric port. Thermal lensing in the recycling cavity optics can also destabilize the angular control system by reducing the sensitivity to certain degrees of freedom and destabilizing the feedback control matrix.

A particular optical design choice exacerbated some of these problems. The recycling cavities were made much shorter (for practical reasons) than the long arms. With the large beams required for low thermal noise, such short cavities are geometrically unstable (cavity g-factor (Siegman, 1986) near unity) (Gretarsson *et al.*, 2007). Small thermal distortions were found to drive the system into instability due to the degeneracy among the higher order spatial modes.

In order to compensate for this effect, active thermal correction systems were installed to smooth out the thermal gradients (Accadia *et al.*, 2010b; Ballmer, 2006; Lawrence *et al.*, 2004; Lück *et al.*, 2004; Rocchi *et al.*, 2012) as well as to improve the fringe contrast at the anti-symmetric port.

Due to the troubles with degenerate cavities, the KAGRA and Advanced LIGO detectors are adding extra optics in their design to break the modal degeneracy in the recycling cavities (Arain and Mueller, 2008; Granata *et al.*, 2010a).

VII. SECOND GENERATION DETECTORS

The purpose of the second generation interferometers is to achieve such a strain sensitivity that the detections of gravitational waves should become fairly regular, enabling the use of these detectors as astronomical tools. They are roughly 1 order of magnitude more sensitive than the first generation detectors (cf. FIg. 18). The world-wide network comprised of Advanced LIGO (Harry, 2010; LIGO, 2011), Advanced Virgo (The Virgo Collaboration, 2012; Virgo, 2011),

GEO-HF (Lück *et al.*, 2010), and KAGRA (KAGRA, 2011; Somiya, 2011) will all use power and signal recycling and a variant of tunable resonant sideband extraction.

A. Monolithic Silica Suspensions

The first generation LIGO and Virgo interferometers were somewhat limited by thermal noise in the mirror suspensions. This was partially due to the intrinsic dissipation of the steel wires and partially due to excess friction in the wire attachments (Abbott *et al.*, 2009). In order to avoid both of these problems, the new suspensions are nearly monolithic: instead of a steel pendulum wire, a high quality fused silica (sapphire for KAGRA) fiber is drawn, and then bonded directly to silica attachments on the mirror barrel(Aston *et al.*, 2012; Cumming *et al.*, 2012; Robertson *et al.*, 2002). As most of the elastic energy (and therefore the dissipation) is concentrated near the bending points at the ends (cf. Sec. V.B.2), the cross sectional shape, near the ends, is optimized with respect to the noise (**?**). This type of silica suspension has been used in the GEO600 and Virgo+ interferometers.

FIG. 9: (Color online) Advanced LIGO Quadruple suspension. The final stage is a 40 kg mirror suspended by four laser-welded silica fibers.

As with the mirror coatings (Sec. V.B.1), both the dissipation due to internal friction as well as the thermoelastic (Zener) damping need to be considered. For highly stressed fibers, one must also consider the temperature dependence of the Young's modulus (dY/dT): the fundamental thermodynamic temperature fluctuations which produce the usual thermoelastic noise via the thermal expansion coefficient also drive the stressed suspension fiber by changing the Young's modulus (Cagnoli and Willems, 2002). Fortuitously for LIGO and Virgo, fused silica has a positive dY/dT; the result is that an appropriate fiber diameter can be chosen to cancel these thermoelastic effects.

Finally, studies of the fiber's mechanical loss as a function of fiber dimension have revealed that the Q is limited by defects in the fiber's surface (Gretarsson and Harry, 1999; Gretarsson *et al.*, 2000; Hammond *et al.*, 2012; Heptonstall *et al.*, 2010; Penn *et al.*, 2006) and not by the intrinsic mechanical dissipation of fused silica. Several decades of experience with surface treatment of quartz oscillators and quartz fibers have informed the current design for GW detectors. The fibers which are now used for the Advanced LIGO mirrors are pristine with a small concentration of residual defects in the surface. These defects in addition to the losses in the welded attachment point dominate the Brownian thermal noise in the suspension. Techniques for evading this limit for the next generation are described in Sec. VIII.D.

B. Mirror Metrology

To support Gaussian beam shapes in the Fabry-Perot cavities, the mirrors are polished to have spherical profiles. Deviations from the ideal shape reduce the overall interferometer performance in a number of ways. Roughly speaking, perturbations at small spatial scales promptly scatter light out of the cavity. Larger scale defects distort the ideal TEM_{00} eigenmode of the arm cavities. To compute the power lost into wide angles, one needs only to know the bidirectional reflectance distribution function (BRDF)(Bass and Mahajan, 2009) of the mirror which is readily obtained from measurements of the mirror surface map (Walsh *et al.*, 1999; Yamamoto, 2007). To first order, this distinction between small and large scales can be made in the following way: light scattered from a mirror which falls off the opposing mirror of the cavity is lost and does not contribute to the cavity mode distortion. In the LIGO case this corresponds to an angle of $\theta_{lost} \sim r_{mirror}/(L_{FP})$ and a spatial scale of $x_{rough} \sim \lambda/\theta_{lost} \sim 2\,\mathrm{cm}$.

For the larger spatial scales the situation is complex; the scattered field is captured on the far mirror and so it is not precisely 'lost'. Rather, the resulting distortion in the cavity field results in an imperfect interference at the Michelson anti-symmetric port. At the smaller scales,

however, a good approximation for the power lost due to surface roughness is

$$\frac{P_{scatter}}{P_{incident}} = \left(\frac{4\pi\sigma}{\lambda}\right)^2 \tag{17}$$

where σ is the RMS surface roughness and λ is the laser wavelength. Finally, at the smallest scales the dominant source of the loss is a random distribution of point scatterers. The ultimate nature of these points has not been discovered as of this writing; the common wisdom is that they are density or index defects in the dielectric coatings. The scatter from these points is therefore treated as either Rayleigh or Mie scattering (depending upon the defect size).

Power loss limits the maximum achievable power recycling buildup, reduces the maximum benefits achievable from QND techniques by degrading the quantum entanglement of the light (cf. Sec. VIII.A.4), and introduces technical noise from backscatter (cf. Sec. V.A.3). Over the past decade, an intense development effort has led to improvements in the mirror polish on both long and short scales. The combination of extremely accurate metrology (Sykora and de Groot, 2011) of the mirror profile and the use of ion beam figuring has resulted in an order of magnitude smoother mirror (see Fig. 10) than the first generation GW interferometers.

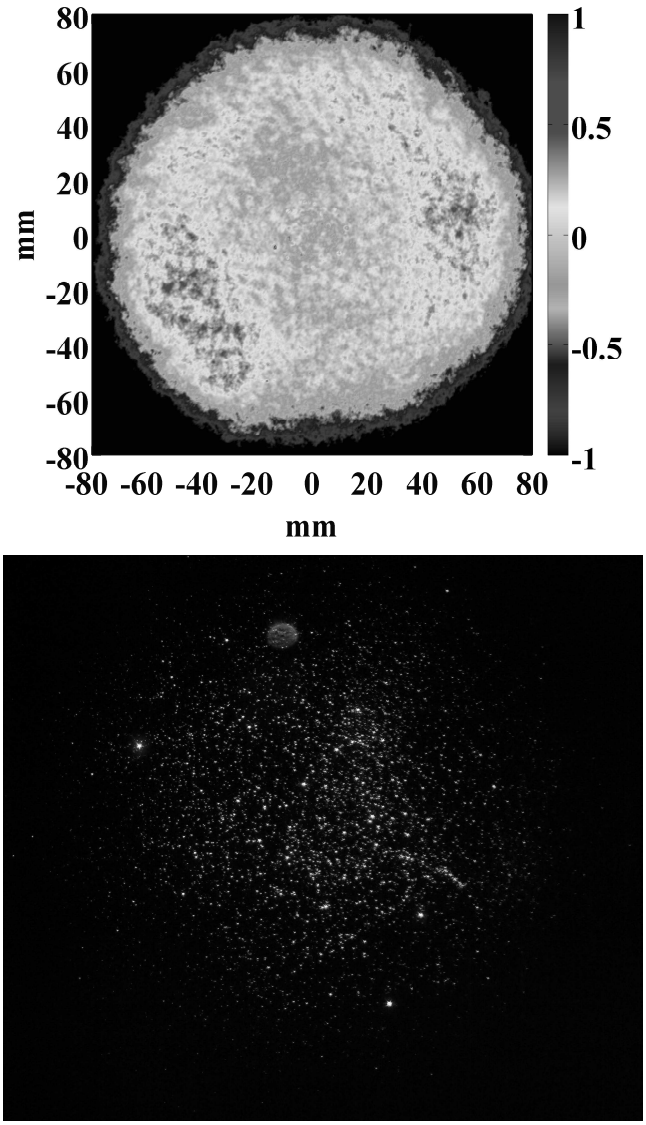

FIG. 10: (Color online) (top) Surface phase map (in units of nm) of one of the Advanced LIGO arm cavity mirrors after applying the high reflectivity mirror coatings (ZygoEPO, 2011). (bottom) infrared image of an initial LIGO arm cavity mirror taken with the cavity locked, highlighting the abundance of point defects. The red oval is the diffuse scatter from an auxiliary beam used for tracking the mirror angle.

C. Dual Recycling

The dynamic tuning capability of signal recycled interferometers is a powerful one and makes these instruments qualitatively different from their predecessors. By adjusting the length of the signal recycling cavity by fractions of a wavelength, the coupled resonance between the arm cavities and the signal mirror can be fine-tuned to match the frequency content of astrophysical sources as shown in Fig. 12. The low frequency response is due to the radiation pressure induced optical spring (cf. Sec. V.A.1) and can also be tuned by adjusting the laser power. Both the signal mirror position and the laser power can be adjusted remotely to arrive at a new configuration within minutes, in principle.

The baseline configuration of the Virgo and KAGRA interferometers will have the signal recycling cavity slightly detuned from resonance in order to maximize the sensitivity to a specific astrophysical source: the inspiral of a binary neutron star system ($M_1 = M_2 = 1.4\,M_\odot$). The Advanced LIGO and GEO-HF interferometers will begin operation in a broadband resonant sideband extraction configuration.

l. Mode Healing In addition to the ability to tune the response of the interferometer to the spacetime strain, the interferometers with signal recycling cavities also exhibit the phenomenon known as *mode healing* (Heinzel *et al.*, 1998; McClelland *et al.*, 1993). Without this mirror, differences in the spot size or wavefront curvature of the beams from the two Michelson arms result in an imperfect destructive interference at the Michelson antisymmetric port (where the GW signal is recorded). This extra light produces no signal but contributes to extra shot noise as well as introducing technical difficulties with the interferometer control system (Smith-Lefebvre *et al.*,

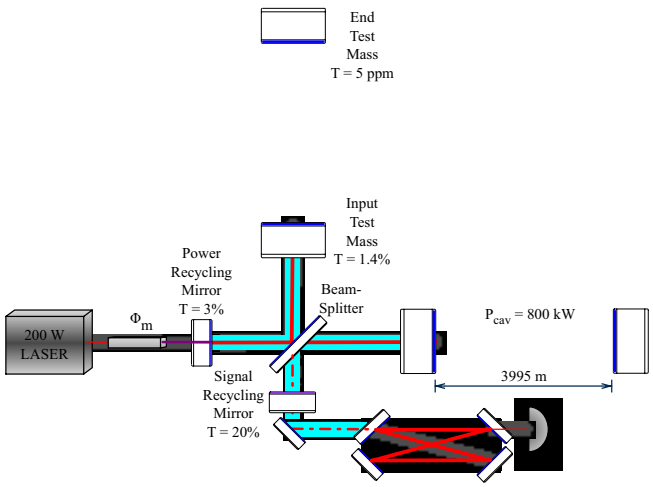

FIG. 11: (Color online) Schematic of the Advanced LIGO interferometers. The output beam at the anti-symmetric port is filtered by a rigid bow-tie cavity to remove the RF sidebands and the higher-order spatial modes which come from distortions in the optics.

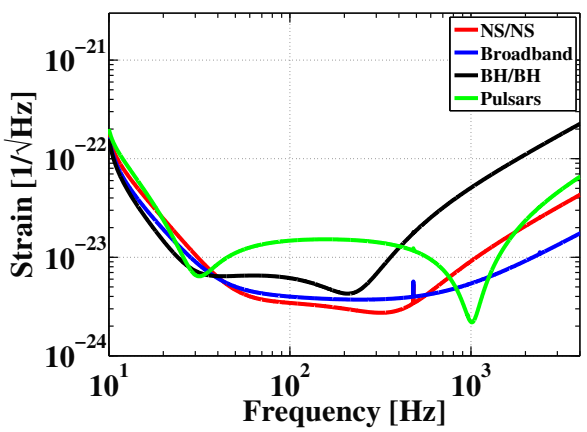

FIG. 12: (Color online) Detector configurations to target particular astrophysical sources. Shown are the optimal tunings of the Advanced LIGO interferometer for (NS/NS) neutron star binary inspirals, (BH/BH) for intermediate mass black hole binary inspirals, and (Pulsars) for narrowband sources (such as pulsars) emitting gravitational radiation around 1 kHz. The Broadband configuration has the best overall sensitivity and is expected to be the easiest to operate.

2011). The signal recycling cavity can be designed to be anti-resonant for this 'junk light' so as to preferentially keep it from getting to the detection port while allowing the signal light to pass (Bochner, 2003; Pan, 2006). With different storage times for each higher order spatial mode, some of the energy which is initially scattered out from the fundamental mode can come back into this mode due to the mode mixing which occurs at each perturbed optical surface. Depending on the details of mirror roughness, signal cavity tuning, and g-factors of the arms and signal cavity, there can be either mode healing or mode harming for the fundamental mode.

D. High Power Opto-Mechanics

These new high-quality optics make it possible to use massively higher power levels. The designs of the Advanced interferometers call for storing 0.5-1 MW in the arm cavities in order to improve the shot-noise limited sensitivity; this is a factor of 10 - 50 higher than the previous generation.

While some differences exist among the laser designs for LIGO, Virgo (Gréverie *et al.*, 2010), and KAGRA, they share a set of common themes. First, a low noise master oscillator (∼1-2 W) is amplified with one or two amplifier stages. The light is then passed through a low finesse cavity in order to filter angular fluctuations and to provide filtering of amplitude noise at RF frequencies.

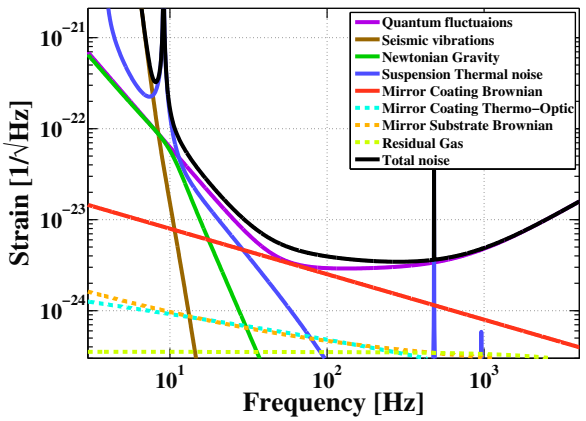

FIG. 13: (Color online) Noise budget of the Advanced LIGO interferometers operating in a Broadband configuration with the parameters of Table III.

The LIGO design has a 2 W Innolight NPRO as the master oscillator, followed by a single pass power amplifier with an output of 35 W. This configuration was used as the laser for the Enhanced LIGO (Fricke *et al.*, 2012). This 35 W system has now been augmented by a high power stage to produce 200 W of single mode light at 1064 nm (Willke *et al.*, 2008).

With the direct (homodyne) readout scheme adopted for LIGO, Virgo, GEO, and KAGRA, the laser power fluctuations show up directly in the readout signal. At high power levels, the dominant coupling path for laser power fluctuations is not so direct. The classical radiation pressure from the laser power fluctuations pushes the mirrors directly and couples to the anti-symmetric port through the imbalance in the finesse of the arm cavities. To mitigate this somewhat, multi-stage active stabilization is used to suppress the raw laser noise by several orders of magnitude. In the end, the relative power stability

Detector	KAGRA	GEO-HF	Adv. Virgo	Adv. LIGO
Arm Length [m]	3000	600	3000	3995
Mirror Mass [kg]	27	5.5	40	40
Beam Spot Size [cm]	3.5	2.4	6	5.9
# of seismic stages	1 + 5	1 + 3 + 3	1 + 6	1 + 2 + 4
Stored Power [kW]	400	10	760	800
Strain Noise $[10^{-23}/\sqrt{\text{Hz}}]$	0.3	3.5	0.3	0.3
Sensitive Band [kHz]	0.02-3	0.1-5	0.02 - 3	0.01 - 5
Location	Japan	Germany	Italy	USA

TABLE III: Comparison of 2nd generation interferometers (KAGRA (Somiya, 2011), GEO-HF (Lück *et al.*, 2010), Advanced Virgo (The Virgo Collaboration, 2009, 2012), and Advanced LIGO (Harry, 2010; LIGO, 2011)). The numbers in the seismic row refer to the number of external active, internal passive, and pendulum suspension stages, respectively.

of the light entering the interferometer is $\lesssim 10^{-8}/\sqrt{\text{Hz}}$ in the GW band (Kwee *et al.*, 2009).

The sensitivity to laser frequency noise is expected to be no greater than it was for the first generation detectors. Therefore, the same strategy of using a multi-stage active stabilization scheme (Abbott *et al.*, 2009; Acernese *et al.*, 2009; Fritschel *et al.*, 2001) is expected to be sufficient.

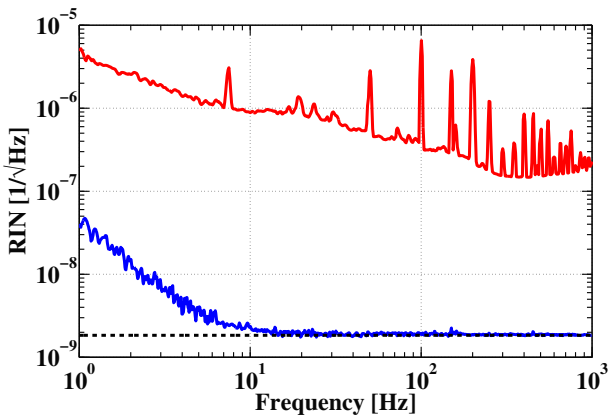

FIG. 14: (Color online) Relative power fluctuations after stabilization of a prototype laser system: (RED) free running laser noise, (BLUE) stabilized level (out of loop), (BLACK) shot noise limit. The goal for Advanced LIGO is $2 \times 10^{-9}/\sqrt{\text{Hz}}$.(Kwee *et al.*, 2009)

1. Angular Instabilities

In 2002, the LIGO interferometers were beset by weak angular instabilities as the stored powers in the arm cavities exceeded $\sim 1\,\text{kW}$. Sidles and Sigg pointed out (Sidles and Sigg, 2006) that these instabilities must be due to radiation pressure overwhelming the mechanical restoring torques of the mirror suspensions.

The mechanism behind this 'Sigg-Sidles' instability is illustrated in Fig. 15. In this picture the radiation pressure couples the suspended optics at either end of the

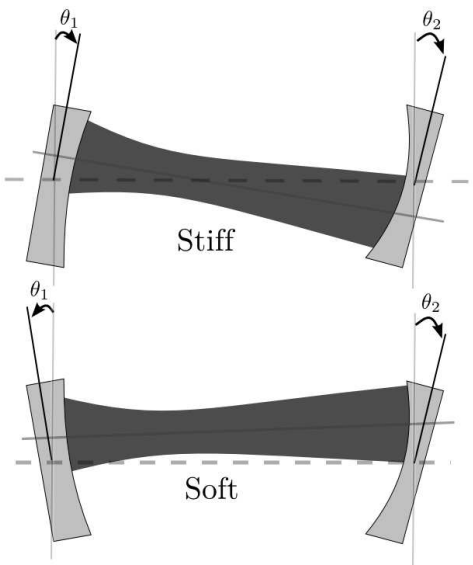

FIG. 15: (Color online) The common and differential angular modes of the Fabry-Perot cavity mirrors are softened (bottom) and stiffened (top) by the radiation pressure torque.

cavity. Including this optical torque, the two mirror system can now be seen as having a 'soft' and 'stiff' mode. With enough stored optical power, the radiation pressure torque can statically de-stabilize the cavity in the soft mode.

In the individual mirror angle basis, we can define an optical torsional stiffness matrix:

$$\kappa_{RP} = \frac{2P}{c}\frac{L}{1-g_1 g_2}\begin{pmatrix} -g_2 & 1 \\ 1 & -g_1 \end{pmatrix} \tag{18}$$

where P is the cavity power, L is the cavity length, and the cavity g-factors for each mirror are defined as $g_i = 1 - L/R_i$, where R_i is the radius of curvature of the i^{th} mirror. The cavity instability occurs when the eigenvalue from this torsional matrix corresponding to

the 'soft' mode overwhelms the mechanical torsional stiffness of the mirror suspension.

As described in Sec. V.B.1, the cavity beam sizes are maximized to reduce the impact of the mirror's thermal noise. This has the unfortunate side-effect of amplifying these optical torsional stiffnesses. The large beam sizes can be realized by utilizing either a plane-parallel or concentric cavity design (Siegman, 1986). As can be seen from Eq. 18, the concentric design (which has negative g-factors) causes the dominant mode to have a positive sign and thereby contribute to the 'stiff', self-aligning mode. The plane-parallel design, on the other hand, has positive g-factors. In this case the denominator of Eq. 18 blows up as the g-factors approach unity (as they must to increase the spot sizes). For this reason, the concentric design has been adopted for all modern GW detectors.

This 'Sigg-Sidles' effect was first characterized for the initial LIGO detectors (Hirose *et al.*, 2010) and then subsequently in the Enhanced LIGO where a modal control approach was used to stabilize it (Dooley, 2011). This modal approach seems to be sufficient to control the instability (Barsotti *et al.*, 2010) but the noise from the control system is likely to be comparable to the more fundamental limits (e.g., suspension thermal noise).

2. Parametric Instabilities

With high circulating powers in the arm cavities, a parametric instability can occur involving the high-Q mechanical modes of the mirrors and higher order transverse optical modes of the Fabry-Perot cavity (Braginsky *et al.*, 2001, 2002; Strigin and Vyatchanin, 2007). Although not observed in the first generation detectors, similar instabilities have been observed in toroidal microcavities (Kippenberg *et al.*, 2005) and in short, kilogram-scale Fabry-Perot cavities (Corbitt *et al.*, 2006).

Following (Evans *et al.*, 2010) we can write the round-trip parametric gain for the m^{th} mechanical mode as:

$$R_m = \frac{4\pi Q_m P}{M\omega_m^2 c\lambda} \sum_{n=0}^{\infty} \Re\{G_n\} B_{m,n}^2 \qquad (19)$$

where Q_m is the mechanical Q of the mode, P is the arm cavity stored power, M is the mirror mass, ω_m is the mechanical eigenfrequency, λ is the laser wavelength, $B_{m,n}$ is the overlap coefficient between the mechanical mode and the optical mode, and G_n is the round trip gain for the scattered field within the entire interferometer.

Even considering the optical resonance of the full interferometer, predicting the impact of parametric instabilities is difficult. The details of the surface figure for each of the mirrors shifts the resonant frequency for the higher order optical modes by a significant fraction of the cavity linewidth. Small differences in dimensions of mirrors and long term drifts in the laboratory temperatures can make order of magnitude changes in the round trip gain by reducing the frequency overlap between the mechanical and optical modes.

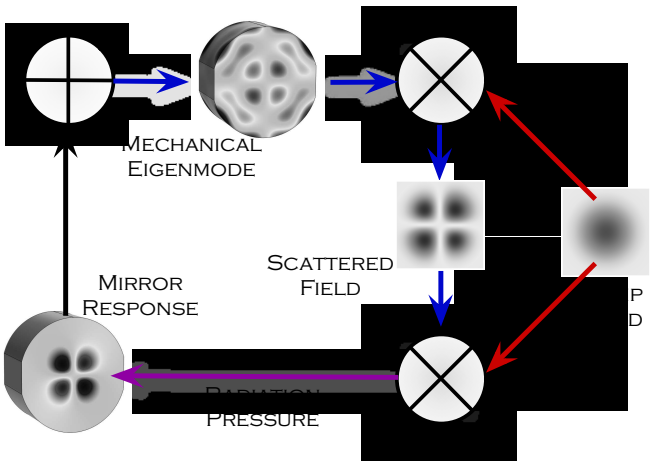

FIG. 16: (Color online) Feedback loop diagram of the parametric instability process. The oscillation of one of the mirror's mechanical eigenmodes scatters the resonant cavity mode into a higher order tranverse mode which resonates partially in the coupled optical cavities of the interferometer and returns to excite the mirror via radiation pressure.

A Monte Carlo analysis (Evans *et al.*, 2010) indicates that there is likely to be ∼several unstable modes in a full power Advanced LIGO interferometer. As the masses, Q's, and power levels are similar, most likely the same problems will afflict the Advanced Virgo and KAGRA interferometers.

Several mitigation strategies have been proposed to suppress these instabilities: adding passive damping films to the mirror 'barrel' (Gras *et al.*, 2009), attaching a resonant electro-mechanical damper, active feedback via the existing mirror actuators (Miller *et al.*, 2011) or using the radiation pressure of an external laser (Ju *et al.*, 2009). While there are challenges to be overcome with all of these techniques, it seems likely that a combination of them will be able to suppress the instabilities down to the nuisance level. Future interferometers should be able to scale the mirror mass directly with laser power and thereby stay at a nearly invariant instability level.

E. Low Frequency Seismic Isolation

The experience with the initial interferometers highlighted the multitudinous ways in which large, low-frequency seismic motions can produce noise in the GW signal band through nonlinear upconversion (see Sec. VI.C above). As a result, all of the 2nd generation vibration isolation systems seek to reduce motions not only in the GW band, but also in the 0.01-10 Hz band.

The Advanced LIGO system is a 3-stage hybrid, active-passive platform (Abbott *et al.*, 2002). There is a hydraulic pre-isolator to provide coarse positioning and

FIG. 17: (Color online) Advanced LIGO Vibration Isolation platform: this double stage, in-vacuum platform provides active isolation from 0.5-30 Hz and passive isolation above ∼1 Hz. The leaf springs around the outer edge of the image provide the vertical compliance. The copper coils near the center of the image are part of the coil-magnet actuators used in the active feedback. Inertial sensors in sealed pods are attached to the platforms to provide the readbacks in the isolation servos.

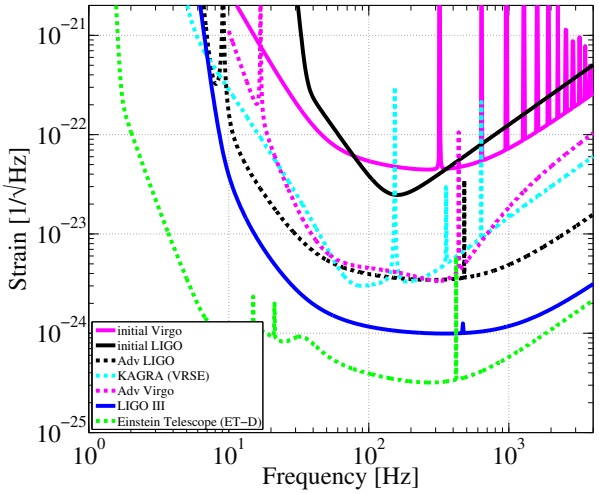

FIG. 18: (Color online) Comparison of strain noise estimates for the ground based detectors. The 'LIGO-III' trace refers to an upgrade of the Advanced LIGO detector including several of the ideas mentioned in Sec. VIII.

coarse active vibration control. This is followed by 2 compliant platforms which provide passive isolation above ∼1 Hz and active isolation from 0.1-30 Hz. An array of seismometers placed near each mirror will be used to reduce the fluctuations in the low frequency, global interferometric lengths (DeRosa *et al.*, 2012) that arise from the microseismic peaks (Giaime *et al.*, 2003).

A comparison of the vibration isolation performance of all ground based GW detectors is shown in Fig. 5.

VIII. THIRD GENERATION DETECTORS

Even conservative estimates of astrophysical event rates (Abadie *et al.*, 2010; Cutler and Thorne, 2002; Phinney, 1991) predict many detections per year for the second generation detectors. Once the first detections are well established, one would like to move on to using the waveforms to make tests of astrophysical models, use 'standard' sirens for high precision cosmography, and make tests of fundamental physics (Punturo *et al.*, 2010). In order to pursue this type of science, the sensitivity must be pushed beyond what the second generation detectors are capable of.

A combination of astrophysical motivations and technical developments has driven the European design of the Einstein Telescope (Einstein Telescope Science Team, 2011; Sathyaprakash *et al.*, 2012). The Einstein Telescope (ET) is foreseen to be an underground, triangular, 10 km interferometer array operating at cryogenic temperatures. The goal is to improve upon the broadband sensitivity by an order of magnitude over the 2$^{\rm nd}$ generation instruments and to move the lower frequency cutoff by a factor of 2-3. The most recent estimates of the ET sensitivity goal are shown in Fig. 18.

The LIGO Scientific Collaboration is currently studying the possibility of a complementary 3$^{\rm rd}$ generation detector network. As the LIGO detectors have yet to reach the fundamental limits of the existing facilities, the study focuses on implementing the new interferometers in the existing vacuum system.

In the following sections, several of the key techniques to making this improvement are described.

A. Quantum Non-Demolition

Most of the noise limits for the large interferometers have already been reduced to below the usual quantum limits (cf. Fig. 13). Improving the quantum limits will give a larger scientific payoff than any other technical improvement. Correspondingly, there has been an explosion of research into Quantum Non-Demolition (QND) readout schemes for GW interferometers in the 21st century. Here we will just describe several of the most promising ideas (Braginsky and Khalili, 1996).

Recent reviews of the state of the art in QND for GW detectors describes well some of the more promising techniques (Chen, 2013; Chen *et al.*, 2010; Corbitt and Mavalvala, 2004; McClelland *et al.*, 2011; Schnabel *et al.*, 2010). In the past decade, there has been a number of theoretical and experimental advances which have lead to better estimates of what is possible. We can categorize the basic optical topologies in the following way:

1. Frequency Dependent Squeezed State Injection

The injection of squeezed light has long been seen as a panacea for the quantum noise limits of GW detection. However, the direct injection of squeezed light can only reduce the noise in the quadrature which has been squeezed (Caves and Schumaker, 1985); phase-squeezed light would improve the shot noise limited region, but add, *at least*, a corresponding amount of radiation pressure noise. Work by (Kimble *et al.*, 2001) and later by (Harms *et al.*, 2003) showed that kilometer sized cavities could be used to apply a frequency dependent phase shift to the squeezed fields. This phase shift can be tuned to provide amplitude squeezing in the band where the radiation pressure is dominant and phase squeezing where the shot noise dominates. For the broadband (tuned-RSE) configuration of Advanced LIGO, this can be accomplished with a single cavity. For the detuned-RSE configurations chose by Virgo and KAGRA, two cavities are required to optimally match the squeeze quadrature to the interferometer's opto-mechanical response.

Following early work on producing squeezed states at high frequencies (Wu *et al.*, 1986), the GW community pushed the technology to produce high levels of squeezing at audio frequencies (Chua *et al.*, 2011; Mckenzie, 2008; McKenzie *et al.*, 2004; Stefszky *et al.*, 2012; Vahlbruch *et al.*, 2006) on table-top prototypes. In the last few years, moderate levels of noise improvement have been observed from injecting squeezed light into a suspended prototype (Goda *et al.*, 2008) as well as the GEO600 (LIGO Scientific Collaboration *et al.*, 2011) and Enhanced LIGO (Abadie *et al.*, 2012; Dwyer, 2012) detectors.

With the confidence gained from these demonstrations and the imminent prototyping of quadrature rotating filter cavities, it is very likely that the 2^{nd} generation detectors can be upgraded with the injection of squeezed states of light before the end of the decade.

2. Frequency Dependent Readout Quadrature

The quantum correlations built up in the signal recycled interferometers make it possible to surpass the Standard Quantum Limit in a narrow band (Buonanno and Chen, 2002; Vyatchanin and Matsko, 1996). At high power levels, the vacuum fields in the amplitude quadrature drive the mirror and produce signals in the phase quadrature as well. By choosing the appropriate combination of homodyne readout quadratures after the photodetection, the amplitude noise can be partially cancelled.

The addition of one of the long quadrature rotation cavities can allow one to rotate the *readout* quadrature as a function of frequency and cancel the sensitivity to the radiation pressure noise (Khalili, 2007; Kimble *et al.*, 2001). The radiation pressure noise itself has not been cancelled; the mirrors are still moving. Rather, we have just chosen to adjust the phase of our optical readout so as to ignore such perturbations. This technique is often referred to as the *variational readout* technique. However, this delicate cancellation by tuning of the readout quadrature has its problems: optical losses in the rotation cavity degrade this scheme faster than the squeezed light injection scheme above. Since the cancellation also subtracts much of the signal, it becomes more sensitive to any degradation of the internal squeezing due to losses.

3. QND Observable Readout

In the Heisenberg picture, the increase in our positional resolution comes at the expense of increased momentum perturbations since the position and momentum do not commute. The momentum perturbations influence the time evolution of the mirror position and spoil the low frequency sensitivity. An alternative to this approach is to read out some observable which carries the gravitational wave information and also commutes with itself at later times. In this way, we would have a true QND observable readout and not have to worry about the quantum back-action effects (Braginsky and Khalili, 1999). One such observable is the mirror's momentum (or speed) (Braginsky *et al.*, 2000; Purdue and Chen, 2002). Practically, this can be done by adding one of the long filter cavities into the interferometer in such a way so as to differentiate the usual positional signal. By taking the differences between successive position measurements, the readout variable closely approximates momentum and so this type of interferometer is often referred to as a *speedmeter*.

4. Optical Losses and QND

In addition to the squeezing input, the variational readout, and the speedmeter, there are a host of other possibilities for QND upgrades: optical 'levers' (Khalili, 2002), multi-wavelength optical springs (Rehbein *et al.*, 2008), and multi-wavelength 'xylophones' (Rehbein *et al.*, 2007), etc. The issues with most of the previous inter-comparisons is that they do not include losses in a realistic way. In addition to the optical losses due to scattering within the interferometer, losses in the readout chain, and finite quantum efficiency of photodetectors, one must also include the losses in the quadrature rotating filter cavities. To include these losses in a realistic way, it is important to remember that the true loss will scale with the beam size (cf. Sec. VII.B) and thereby the cavity length.

A numerical comparison which incorporates realistic losses within the framework of the 'LIGO-III' design has

Parameter	Symbol	Value	Units	Parameter	Symbol	Value	Units
Light Wavelength	λ	1064	nm	Substrate Young's Modulus	Y_{sub}	185	GPa
Arm Cavity Mirror Mass	m	145	kg	Suspension Ribbon Young's Modulus	Y_{si}	130	GPa
Arm Cavity Length	L	4000	m	Suspension Ribbon Thickness	h_{sus}	0.2	mm
Arm Cavity Finesse	F	550	-	Suspension Ribbon Width	d_{sus}	2	mm
Arm Cavity Power	P_{cav}	3000	kW	Substrate Loss Angle	ϕ_{sub}	3×10^{-9}	rad
Beam Radius	ω	5.8	cm	Coating Loss Angle	ϕ_{coat}	2×10^{-5}	rad
Detection Efficiency	η	0.95	-	Mirror Coating	-	GaAs:AlAs	-
Squeeze Factor	R	10	dB				
Filter Cavity Length	L_{fc}	100	m	Newtonian Noise Sub. Factor	$\aleph_{NN}$	30	-
Filter Cavity R.T. Loss	A_{fc}	33	ppm	Mirror / Suspension Temperature	T	120	K

TABLE IV: Nominal values of some LIGO-III interferometer parameters used for Fig. 20

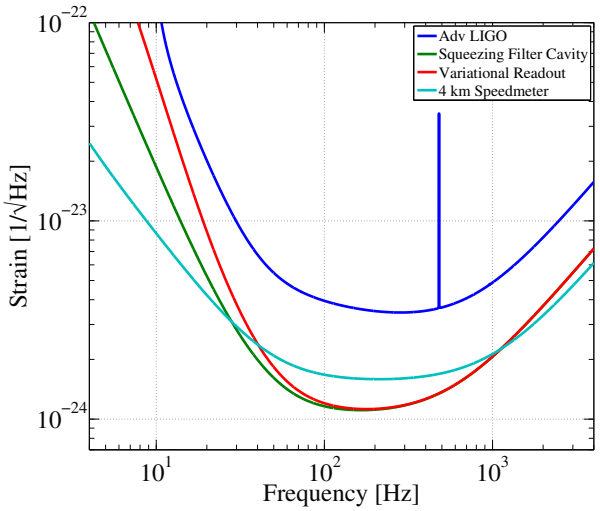

FIG. 19: (Color online) Comparison of the equivalent strain noise levels of various quantum non-demolition schemes implemented on this 'LIGO-III' concept. 10 dB squeezed light is injected in all cases. For the 'Filter Cavity' trace, squeezed light is filtered with a 100 m cavity. For the 'Variational' trace, the output of the interferometer is filtered by a 100 m filter cavity, and for the speedmeter case, the 'Filter Cavity' configuration is modified by adding a 4 km speedmeter cavity.

been carried out by (Miao *et al.*, 2013) and is shown in Fig. 19. Here it has been assumed that the round-trip losses in the filter cavity are 30 ppm (consistent with the past experience about large cavities).

B. Circumventing Mirror Thermal Noise

The relatively large mechanical dissipation in the mirror coatings and the shallow frequency dependence of the resulting mirror surface fluctuations makes the coating thermal noise one of the most serious limits for future detectors. Broadly speaking, two approaches are being pursued to avoid this limit: new coatings with higher mechanical Qs and alternative optical cavity mode shapes which can partially reject the noise.

1. Non-Gaussian Beam Shapes

A straightforward approach to reducing the effects of coating thermal noise is to increase the beam size (cf. V.B.1). However, as described in Section VII.D.1, this can exacerbate the radiation pressure induced angular instability. Even if this can be compensated by an exceptionally sophisticated feedback control system, it is unlikely that beam size alone will offer more than a factor of two improvement in the long run.

A more effective approach might be using higher order spatial modes of the cavity. The field inside of a Fabry-Perot cavity with spherical mirrors can be well approximated with the set of orthonormal Laguerre-Gaussian functions (Siegman, 1986). Within the Virgo project (Vinet, 2010), it has been proposed to use axially symmetric Laguerre-Gaussian modes (chiefly the $LG_{3,3}$ and the $LG_{5,5}$ modes).

In addition to the technical difficulties associated with generation (Granata *et al.*, 2010b) and control (Chelkowski *et al.*, 2009) of such beams, a stability analysis of the cavities (Hong *et al.*, 2011) shows that the cavity field is strongly distorted when taking into account the realistic surface imperfections (see Fig. 10) of the best available mirrors. The several-fold degeneracy of these higher order modes is weakly split by the surface deformations and all of the degenerate modes are partially resonant. In this perturbed state, the fields from the two arm cavities are no longer well-matched and this degrades the interference at the anti-symmetric port of the Michelson. Consequently, the ability to make a low phase noise optical readout is compromised.

An even more complicated option is to use a particular linear combination of Laguerre-Gaussian modes. The so-called 'Mesa beams' (D'Ambrosio *et al.*, 2004; Miller *et al.*, 2008; Tarallo *et al.*, 2007) are one such combination. Simulations (Hong *et al.*, 2011) show that they are

not much worse than $TEM_{0,0}$ Gaussian modes in their susceptibility to angular instabilities or modal degeneracy. Unfortunately, it is not yet straightforward to produce the non-spherical mirrors required for Mesa beams.

The theoretical maximum improvement from any of the above beam shaping techniques is $\sim$ 70%. To make any further improvements it will be necessary to either have radical improvements in the mechanical loss of mirror coatings or build a much longer interferometer.

2. Heteroepitaxial Bragg Mirrors

As described in Sec. V.B.1, the thermal fluctuations of the mirror surface are dominated by the Langevin thermal forces generated in the high-reflectivity dielectric coatings. It has been shown (Phillips, 1987; Pohl *et al.*, 2002) that the mechanical dissipation (and consequently the thermal noise) of nearly all amorphous, thin-film materials is higher than that of crystalline materials. The cause of the dissipation, almost universally, is known to be due to the presence of a set of low energy modes (which are not 'frozen-out'). Tunneling into this vast sea of available modes leads to the observed mechanical dissipation. Of all amorphous solids, fused silica seems to be singular in its extremely low dissipation at room temperature and above (Ageev *et al.*, 2004). Unfortunately, this high Q of the bulk material does not translate into high Q for the silica thin films used in the optics industry.

The poor mechanical Q of amorphous materials leads one towards crystalline coatings. Epitaxial deposition techniques (e.g., chemical vapor deposition, molecular beam epitaxy, atomic layer deposition) have advanced dramatically over the past several decades to support the development of electronic circuits and opto-electronics.

A promising set of prospects are trinary AlGaAs layers grown on GaAs substrates and then attached to silica or silicon mirrors via epitaxial liftoff (ELO) (Demeester *et al.*, 1993). These structures have been grown on GaAs substrates and the resulting mechanical Q is $\sim 30\times$ larger than the best amorphous high reflectivity coatings (Cole *et al.*, 2008). Another possibility is to grow AlGaP:GaP (Lin *et al.*, 2011) layers directly onto silicon substrates where the lattice matching is quite good. The matching may largely mitigate the thermal stresses and allow operation of the interferometer at cryogenic temperatures where the thermal noise is further reduced. If the mechanical dissipation can be maintained at such low levels after ELO and the absorption can be reduced to $\lesssim 5$ ppm, these epitaxial coatings have the promise of expanding the astrophysical reach of the detectors by a factor of 3-10 in the most critical frequency band.

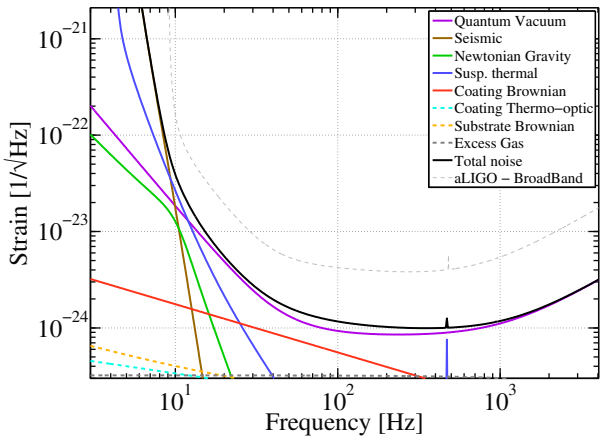

FIG. 20: (Color online) Limiting noise sources for a potential 3rd generation LIGO detector with 3 MW of arm cavity power, 10 dB of frequency dependent squeezed light injection, 140 kg Si mirrors with GaAs coatings operating cryogenically at 120 K, and 30× subtraction of Newtonian gravity noise.

C. Newtonian Gravity Noise Subtraction

As described in Sec. V.B.4, the fluctuations in the local gravitational field will limit any further progress below ∼20 Hz due to the inability to shield the mirrors from local gravitational perturbations. The seismic noise shown in Fig. 4 indicates that the situation is largely the same for LIGO and Virgo, while the Newtonian noise may be as much as an order of magnitude smaller for KAGRA. Underground detectors such as KAGRA and the Einstein Telescope should be designed to have a high degree of symmetry in the shape of the caverns around each test mass. The symmetry of these caverns can then passively cancel much of the Newtonian gravity noise Although it is not possible to significantly reduce the ambient vibrations, it is possible, in principle, to subtract this gravitational noise either by applying canceling forces on the mirrors or by regressing it from the data stream offline.

Clearly the major impediment to subtracting out noise sources, in general, is to determine what part of the interferometer output is noise and what part is signal. If this was straightforward, then all of the important noises could be removed in this manner. The distinguishing feature of the Newtonian noise, however, is that the source terms are readily measured. As we can see from Fig. 6, the dominant component comes from the ambient ground motion in the vicinity of the test masses. Of the various modes of the ground, the chief contributors to the gravitational noise are the Rayleigh waves (Beccaria *et al.*, 1998b; Hughes and Thorne, 1998) on the surface. The body waves in the ground only produce small density perturbations and are at least 10× smaller in their gravitational impact.

In principle, an array of seismometers near each mirror

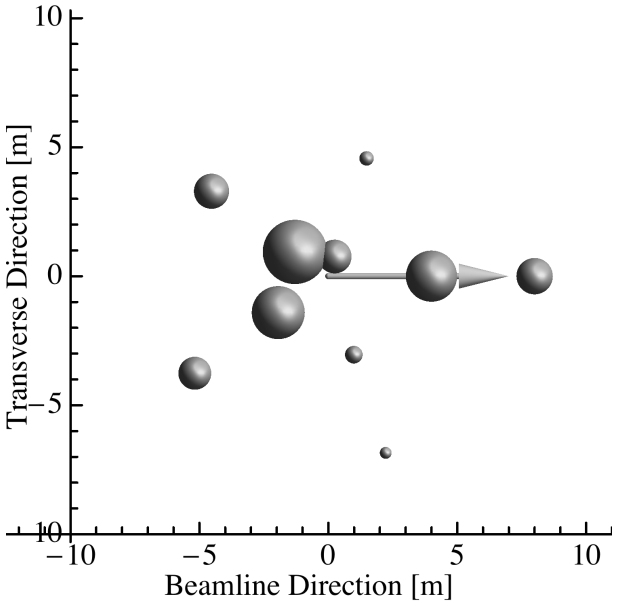

FIG. 21: An example spiral array optimized for subtracting Newtonian noise due to surface waves (Driggers *et al.*, 2012b) for the 'LIGO-III' concept showin in Fig. 20. The center of each sphere indicates the location of one seismometer and the size of the sphere is proportional to the coherence between the seismometer and the Newtonian gravitational perturbations on the test mass. In this plot, the test mass is at (0, 0) and the laser beam direction is indicated by the arrow.

could measure this surface wave contribution. Given the time series of seismic noise, the remaining step is to then determine the Green's function which relates the motion of each sensor to the mirror motion. Given sufficient knowledge about the ground and the surrounding laboratory environment this could possibly give some moderate subtraction quality, but would require significant effort to perform the characterization and construct such an elaborate model with any accuracy.

A more promising approach is to use adaptive noise cancellation algorithms to 'learn' the Green's function and apply the resulting digital filters to the data stream (Beker *et al.*, 2011; Haykin, 2002; Huang *et al.*, 2006; Sayed, 2003). This approach has proven to be successful in the laboratory (Driggers *et al.*, 2012a; Leibrandt *et al.*, 2013; Thorpe *et al.*, 2010) in subtracting the direct seismic influences from fixed cavities and suspended interferometers using an array of several low noise seismometers and accelerometers. Moreover, this technique was employed in the recent LIGO Science run (S6) to remove the seismic influence from several of the interferometric degrees of freedom (DeRosa *et al.*, 2012) as well as magnetic field fluctuations at the mains frequencies (Fricke *et al.*, 2012).

Early estimates of the noise at the LIGO sites and simulations of the subtraction systems indicate that ∼10-20 sensors per test mass will be sufficient to subtract 90% of the noise in the 5-20 Hz band (Driggers *et al.*, 2012b). Experience with Advanced LIGO should allow for making improvements to this depending upon the complexity of the seismic fields.

At the low frequencies where Newtonian noise is dominant, the main sources of gravitational waves are expected to be the mergers of intermediate mass ($M \simeq 10 - 1000\,M_\odot$) black holes and the early part of the inspiral for solar mass compact binaries. The implementation of a Newtonian noise subtraction system should eventually allow for localizing the solar mass binaries to within a reasonable window in the sky and allow electromagnetic telescopes to point to the source well ahead of the merger.

D. Beyond Silica Suspensions

In the next generation mirror suspensions, the frontier is not in improving the vibration isolation, but rather it is in reducing the thermal noise due to the suspension fiber. As discussed in Sec. VII.A, the present limit to the mechanical dissipation comes from the residual defects in the surface layer of the silica fibers. From Eqs. 11 and 13 we can see that progress may be made on two fronts: reducing the temperature and reducing the loss.

1. Silicon Suspensions

To reduce the loss it will be necessary to use a material with a very high mechanical Q (e.g., sapphire, silicon, niobium, diamond (Gaidarzhy *et al.*, 2007)) as well as an extremely high quality surface. Fortunately, surface treatments of monocrystalline silicon have advanced dramatically over the past decade. Present day technologies can already produce silicon with 10× less surface loss than fused silica (Nawrodt *et al.*, 2010) and new etching and passivation methods pioneered by the optomechanics community (Borselli *et al.*, 2006) may surpass this limit by another order of magnitude in the coming decade.

A seemingly straightforward option is to simply operate the interferometer at cryogenic temperatures, thereby winning in the thermal noise as $T^{-1/2}$. In addition, cryogenic silicon has many other excellent low temperature properties: the thermal expansion coefficient goes through zero at 18 and 120 K, the thermal conductivity is at least 300× higher than silica (thus reducing thermal gradients and distortions), and, as is the case with many crystalline substances, the mechanical Q increases with decreasing temperature.

With MW level laser power in the Fabry-Perot cavities, extracting heat from the mirrors becomes an issue for low temperature operation. The high thermal conductivity of materials such as silicon and sapphire may

make it possible to extract ∼10 mW of heat through the suspension fibers (Tomaru *et al.*, 2002) before the thickness of the fiber compromises the thermal noise benefits.

At the higher zero crossing temperature of 120 K, the radiative cooling power of a large mirror can exceed ∼10 W. This should make it possible to cool the mirrors entirely by radiation using a cold shield around the suspension. This essentially noiseless approach should allow for the use of 10× higher circulating power in the interferometer while maintaining the thermal noise benefits of low temperature operation. It remains to be seen if the surfaces can be treated in a way so as to have a high emissivity while not spoiling the mechanical Q too much.

2. Electro-Magnetic Suspensions

A natural route to explore is that of eschewing the fiber altogether and using purely magnetic suspension forces (Drever, 1996; Jayawant, 1981). In principle, the lack of any mechanical support element will eliminate the suspension thermal noise contribution to the interferometer displacement noise. Attaching magnets directly to the mirror is likely to lead to too much mechanical dissipation in the attachments and in the magnets themselves. Another possibility is to find a paramagnetic mirror material and to levitate it with strong permanent magnets (Augst and Drever, 2000) although it seems problematic to simultaneously have a large magnetic susceptibility and high mechanical Q. In either case, the mirror must be well shielded from the ambient magnetic field fluctuations and even then, the Barkhausen noise in the permanent magnets could well introduce an insurmountable noise floor. Even superconducting magnetic suspensions may have dissipation (Hammond *et al.*, 2004; Hebard, 1973) due to nearby eddy currents or small normal regions of the material.

Rather than directly levitating the mirror, the magnetic suspension could be used to support an upper stage of a multi-stage suspension system (Varvella *et al.*, 2004). The mirror could then be supported from this magnetically levitated platform by a passive mechanical suspension. Although this approach would not avoid the fiber's thermal noise, it could allow for a very low frequency suspension and concomitant improvement in filtering of seismic noise.

Another option is to instead use electrostatic(Giazotto, 1998; Willemenot and Touboul, 2000) suspensions. This would seemingly avoid the problems due to coupling from ambient magnetic fields. In any case, the passive stability of any such system is forbidden by Earnshaw's theorem and some kind of active feedback must be used to stabilize at least one degree of freedom. The sensitivity of such a sensor limits the ultimate low frequency performance of such a suspension/levitation system, but it may be very useful as an intermediate stage in a compound pendulum system.

IX. LOW FREQUENCY DETECTORS

The gravitational wave spectrum spans twenty decades in frequency: at the lowest frequencies, corresponding to the age of the universe, the polarization of the cosmic microwave background should contain signals from the primordial gravitational waves due to cosmic inflation (Hu and Dodelson, 2002). The nano- to micro-Hertz band is covered by timing of pulsars and artificial satellites (see Sec. III.B). Between the timing measurements and the ground based detectors, the wide 10^{-5} to 1 Hz band will be pursued with space-based interferometers in the near future.

A. Interferometers in Space

Space detectors have tremendous advantages over ground based detectors below ∼5 Hz. Direct seismic vibrations and Newtonian gravitational fluctuations are almost completely absent. All of the proposed space missions, therefore, are designed to focus on sub-Hz frequencies.

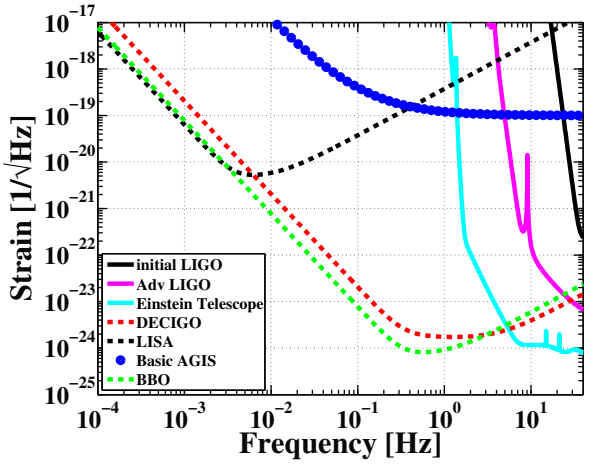

FIG. 22: (Color online) Comparison of strain noise estimates for future detectors: LISA, DECIGO, BBO, Basic AGIS, and ET (D). The LIGO sensitivity curves are included for reference.

1. NGO

NGO (previously LISA: the Laser Interferometer Space Antenna) is a proposed ESA mission (Danzmann and Rüdiger, 2003; Faller *et al.*, 1989; Prince and the LISA Science Team, 2009; Prince *et al.*, 2002) slated for launch in the early part of the 21st century. The design has three

spacecraft flying in a near-equilateral triangle formation in orbit around the sun, trailing the earth by $\sim$ 20°. From each satellite, a laser beam is sent to the others using a large beam expanding telescope. Due to the large distances, most of the light is lost through diffraction, yielding less than 1 nW for detection at each end. The local lasers are then phase locked to this incoming light and sent back to the original satellite similar to standard transponder methods. The phase differences between the lasers contain the GW strain signal as well as various technical noise sources which can be removed by the techniques of Time-Delay Interferometry(de Vine *et al.*, 2010). The low power levels which are received at each satellite result in the interferometer being shot noise limited above a few mHz. Although the expected displacement sensitivity is 'only' $\sim 10^{-11}$ m/$\sqrt{\text{Hz}}$, the impressive strain sensitivity is achieved by having arm lengths of $\sim 10^6$ km. In contrast to the ground-based detectors, NGO will operate in the limit of having many high SNR signals enabling it to do extremely precise tests of astrophysical models and general relativity. In fact, the high sensitivity is expected to lead to a so-called 'confusion noise' limit (Królak *et al.*, 2004) where the low frequency end of the spectrum is dominated by a large foreground of gravitational radiation from galactic and extragalactic compact binaries. In order to reach the sensitivity shown in Fig. 22, sophisticated subtraction algorithms will have to be used in post-processing (Cornish and Porter, 2007). The rotation of the NGO constellation and its orbit around the sun will produce phase and amplitude modulations of the detected signals. These modulations in turn will allow the analysis to reconstruct the angular position of the sources with orders-of-magnitude better resolution than the ground based detectors. Details of the mission technology and science goals can be found in the NGO Yellow Book (NGO, 2013).

2. DECIGO and BBO

Of all of the proposed sources of gravitational radiation, the most exciting one for cosmologists is perhaps the early universe (see Sec. II.B.3). Due to the weak coupling of gravitational waves with matter, a detection of a primordial stochastic background would allow us to peer back into the time when the age of the universe was less than $\sim 10^{-20}$ seconds old. For a scale invariant spectrum of radiation, we have the best chance of detection at low frequencies. Unfortunately, the astrophysical foreground of gravitational waves in the $10^{-9} - 10^{-1}$ Hz band makes the detection of an inflationary background nearly hopeless. Nearly all of the white dwarf binaries have merged before they get to 0.1 Hz (Farmer and Phinney, 2003) and so only the relatively small number of binaries containing neutron stars and black holes remain from 0.1-1 Hz.

Two space missions are being studied to probe this frequency band: the Japanese Deci-Hertz Gravitational-wave Observatory (DECIGO) (Ando *et al.*, 2010b; DECIGO, 2011) and the international Big Bang Observer (BBO) (Cutler and Harms, 2006; Phinney, 2003). In addition to the eventual detection of cosmological backgrounds, there is a wealth of wonderful astrophysical science which can be extracted during the foreground removal of these detectors (Cutler and Holz, 2009; Yagi and Tanaka, 2010). Unfortunately, it is unlikely that either of these missions will fly within the next decade due to budgetary constraints.

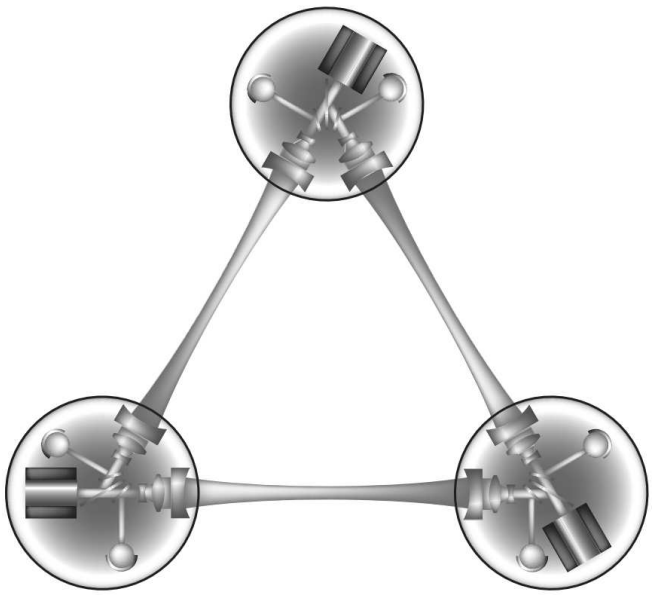

FIG. 23: DECIGO constellation concept (Sato *et al.*, 2009)

B. Low Frequency Terrestrial Detectors

The natural way to avoid terrestrial disturbances is to make an extra-terrestrial detector. However, recent advanced in our understanding of Newtonian gravitational noise have made it reasonable to reexamine this issue. In particular, the relatively higher abundance of sources in the 0.01-10 Hz band and their long duration, make it possible to have astrophysically interesting detectors even if their noise floors are $10^5\times$ higher than that of the km-scale ground based detectors.

1. Torsion Bar Antenna

Recently, a novel arrangement of torsion bars has been proposed to readout sub-Hz gravitational waves (Ando *et al.*, 2010a; Ishidoshiro *et al.*, 2011). The tidal force from an incoming wave will twist the crossed torsion bars differentially. A high sensitivity interferometric sensor is used to read out the differential torsion angle. Early esti-

mates project the strain sensitivity to be near $10^{-19}/\sqrt{\text{Hz}}$ above ~ 0.1 Hz using 10 m bars. With such a sensitivity it should be possible to observe the mergers of intermediate mass black holes out to cosmological distances, search for the merger of galactic white dwarfs (Farmer and Phinney, 2003), and serve as an early warning system for extra-galactic compact object inspirals for the ground based detectors.

2. Atom Interferometers

An alternative to standard laser interferometry is to use clouds of atoms instead of mirrors (Dimopoulos *et al.*, 2008; Hohensee *et al.*, 2011). This method uses pulses of light to change the momentum states of some of the atoms in the clouds. These clouds then take different free fall paths. A final pulse is used to synchronize the momentum states of the atoms and the interference of the atomic clouds is used to read out the GW signal.

The advantages of these atomic techniques are many: the clouds have a very high immunity to radiation pressure noise, very low thermal noise, and no suspension noise. The common launch for the atomic clouds makes the influence of seismic noise nearly zero. However, the Newtonian noise is a problem for the atom interferometers just as it is for laser interferometers.

Bender has highlighted (Bender, 2011; Bender, 2011) several additional complications with the light-pulse atom interferometers which limit significantly the achievable sensitivity; these issues are being addressed by the atomic community (Dimopoulos *et al.*, 2011) It remains to be seen if this type of atom interferometry can be made to be competitive with other technologies (such as DECIGO).

X. CONCLUSION

Many of the most interesting objects in the universe remain invisible so far to those of us on the earth. Our understanding of astrophysics and cosmology has been transformed in the past millenium by observations of electromagnetic radiation, looking into new wavelengths, looking farther back into the early universe, and looking more deeply at our local neighborhood.

We have yet to witness the same revolution through our observations of gravitational radiation and yet the promise for discovery and revolution remains as profound as before.

The recent progress in numerical relativity, wide area astronomical surveys, and gravitational wave detector technology all point to a wonderful convergence of science which will ineluctably lead to another series of revolutions in our understanding of the universe.

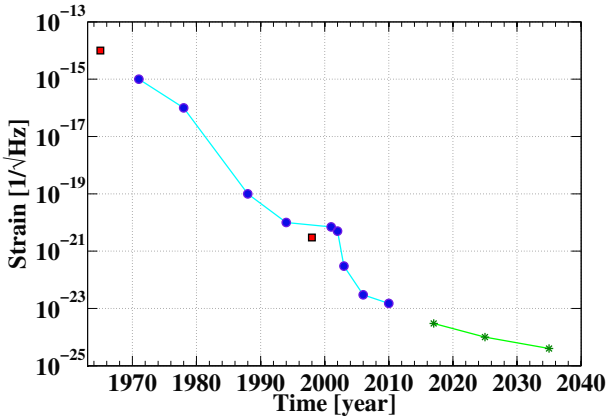

FIG. 24: (Color online) Evolution in gravitational wave detector sensitivity from 1965 into the near future. On the y-axis is plotted the *minimum* of the strain noise spectral density for the given detectors. The acoustic bar detectors are shown as (RED) squares and the laser interferometers as (BLUE) circles. Estimates for future detectors are (GREEN) stars.

The upcoming crop of ground based detectors is almost guaranteed to make detection in the next few years and the laboratory research of today promises to turn the gravitational wave astronomy of the future into a precision science. Buoyed by the likely detections of signals by pulsar timing and terrestrial interferometers, the space missions should complete our coverage of the gravitational wave spectrum. The sources of gravitational waves may often be dark but the future is bright.

ACKNOWLEDGMENTS

I must primarily thank the international community of scientists involved in the search for gravitational waves; I have learned much from them in the last decade.

In particular, I thank H. Grote, H. Lück, D. Tatsumi, K. Arai, M. Barsuglia, L. Barsotti, J. Marque, G. Vajente, and V. Frolov for detailed information on the first generation interferometers and their noise sources. I am grateful to S. Hild, Y. Aso, M. Ando, G. Losurdo, and P. Fritschel for detailed information on the second generation interferometers. I must also thank J. Harms, M. Coughlin, and J. C. Driggers for assembling the updated seismic information from the worldwide network and producing the recent estimates of Newtonian gravity noise, to P. Kwee for the information on the AEI 200 W laser, C. Vorvick for images of the LIGO optic scattering, T. Akutsu for information on DECIGO, W. W. Johnson for elucidation on the sensitivity of bar detectors, S. E. Whitcomb for discussions about excess gas, and to E. K. Gustafson and K. Arai for a careful reading of the manuscript. I gratefully acknowledge the support of the National Science Foundation under grant PHY-0555406.

REFERENCES

Abadie, J., B. P. Abbott, R. Abbott, M. Abernathy, T. Accadia, F. Acernese, C. Adams, R. Adhikari, P. Ajith, B. Allen, G. Allen, E. A. Ceron, *et al.*, 2010, Classical and Quantum Gravity **27**(17), 173001.

Abadie, J., B. P. Abbott, R. Abbott, M. Abernathy, T. Accadia, F. Acernese, C. Adams, R. Adhikari, P. Ajith, B. Allen, G. Allen, E. A. Ceron, *et al.*, 2012, Squeezed light injection in a gravitational wave detector, in prep.

Abbott, B., R. Abbott, R. Adhikari, A. Ageev, B. Allen, R. Amin, S. Anderson, W. Anderson, M. Araya, H. Armandula, *et al.*, 2004a, Nuclear Instruments and Methods in Physics Research Section A: Accelerators, Spectrometers, Detectors and Associated Equipment **517**(1), 154.

Abbott, B., R. Abbott, R. Adhikari, P. Ajith, B. Allen, G. Allen, R. Amin, S. Anderson, W. Anderson, M. Arain, *et al.*, 2009, Reports on Progress in Physics **72**, 076901.

Abbott, B., R. Abbott, R. Adhikari, P. Ajith, B. Allen, G. Allen, R. Amin, S. B. Anderson, W. G. Anderson, M. A. Arain, M. Araya, H. Armandula, *et al.* (LIGO Scientific Collaboration), 2008, Phys. Rev. Lett. **101**, 211102, URL http://link.aps.org/doi/10.1103/PhysRevLett.101.211102.

Abbott, B. P., R. Abbott, F. Acernese, R. Adhikari, P. Ajith, B. Allen, G. Allen, M. Alshourbagy, R. S. Amin, S. B. Anderson, and et al., 2009, Nature **460**, 990.

Abbott, B. P., R. Abbott, R. Adhikari, P. Ajith, B. Allen, G. Allen, R. S. Amin, S. B. Anderson, W. G. Anderson, M. A. Arain, M. Araya, H. Armandula, *et al.*, 2009, Phys. Rev. Lett. **102**, 111102.

Abbott, L., and M. B. Wise, 1984, Nuclear Physics B **244**(2), 541 , ISSN 0550-3213, URL http://www.sciencedirect.com/science/article/pii/0550321384903298.

Abbott, R., R. Adhikari, G. Allen, D. Baglino, C. Campbell, D. Coyne, E. Daw, D. DeBra, J. Faludi, P. Fritschel, *et al.*, 2004b, Classical and Quantum Gravity **21**(5), S915.

Abbott, R., R. Adhikari, G. Allen, S. Cowley, E. Daw, D. DeBra, J. Giaime, G. Hammond, M. Hammond, C. Hardham, J. How, W. Hua, *et al.*, 2002, Classical and Quantum Gravity **19**(7), 1591.

Abramovici, A., W. E. Althouse, R. W. P. Drever, Y. Gürsel, S. Kawamura, F. J. Raab, D. Shoemaker, L. Sievers, R. E. Spero, K. S. Thorne, R. E. Vogt, R. Weiss, *et al.*, 1992, Science **256**(5055), 325.

Accadia, T., F. Acernese, M. Alshourbagy, P. Amico, F. Antonucci, S. Aoudia, N. Arnaud, C. Arnault, K. G. Arun, P. Astone, and et al., 2012, Journal of Instrumentation **7**, 3012.

Accadia, T., F. Acernese, F. Antonucci, P. Astone, G. Ballardin, F. Barone, M. Barsuglia, A. Basti, T. Bauer, and M. G. Beker, 2010a, Astroparticle Physics ISSN 09276505, URL http://dx.doi.org/10.1016/j.astropartphys.2010.10.005.

Accadia, T., F. Acernese, F. Antonucci, P. Astone, G. Ballardin, F. Barone, M. Barsuglia, A. Basti, T. S. Bauer, M. G. Beker, A. Belletoile, S. Birindelli, *et al.*, 2011, Astroparticle Physics **34**, 521.

Accadia, T., F. Acernese, F. Antonucci, P. Astone, G. Ballardin, F. Barone, M. Barsuglia, T. S. Bauer, M. G. Beker, A. Belletoile, S. Birindelli, M. Bitossi, *et al.*, 2011a, Low Frequency Noise, Vibration and Active Control **30**(1), 63.

Accadia, T., F. Acernese, P. Astone, G. Ballardin, F. Barone, M. Barsuglia, A. Basti, T. S. Bauer, M. Bebronne, M. G. Beker, A. Belletoile, M. Bitossi, *et al.*, 2011b, Classical and Quantum Gravity **29**(2), 025005.

Accadia, T., B. L. Swinkels, and V. Collaboration, 2010b, Classical and Quantum Gravity **27**(8), 4002.

Acernese, F., M. Alshourbagy, P. Amico, F. Antonucci, S. Aoudia, K. G. Arun, P. Astone, S. Avino, L. Baggio, G. Ballardin, F. Barone, L. Barsotti, *et al.*, 2008, Classical and Quantum Gravity **25**(18), 184001.

Acernese, F., M. Alshourbagy, F. Antonucci, S. Aoudia, K. Arun, P. Astone, G. Ballardin, F. Barone, M. Barsuglia, T. Bauer, *et al.*, 2010a, Astroparticle Physics **33**(3), 131.

Acernese, F., M. Alshourbagy, F. Antonucci, S. Aoudia, K. G. Arun, P. Astone, G. Ballardin, F. Barone, L. Barsotti, M. Barsuglia, T. S. Bauer, S. Bigotta, *et al.*, 2009, Phys. Rev. A **79**, 053824, URL http://link.aps.org/doi/10.1103/PhysRevA.79.053824.

Acernese, F., P. Amico, M. Al-Shourbagy, S. Aoudia, S. Avino, D. Babusci, G. Ballardin, R. Barille, F. Barone, L. Barsotti, M. Barsuglia, F. Beauville, *et al.*, 2006, IEEE Transactions on Instrumentation and Measurement **55**(6), 1985.

Acernese, F., P. Amico, M. Al-Shourbagy, S. Aoudia, S. Avino, D. Babusci, G. Ballardin, R. Barillé, F. Barone, L. Barsotti, M. Barsuglia, F. Beauville, *et al.*, 2006, Classical and Quantum Gravity **23**, 91.

Acernese, F., P. Amico, M. Alshourbagy, F. Antonucci, S. Aoudia, P. Astone, S. Avino, D. Babusci, G. Ballardin, F. Barone, *et al.*, 2007, Applied Optics **46**, 3466.

Acernese, F., P. Amico, N. Arnaud, D. Babusci, R. Barillé, F. Barone, L. Barsotti, M. Barsuglia, F. Beauville, M. A. Bizouard, C. Boccara, F. Bondu, *et al.*, 2004, Classical and Quantum Gravity **21**, 433.

Acernese, F., F. Antonucci, S. Aoudia, K. Arun, P. Astone, G. Ballardin, F. Barone, M. Barsuglia, T. Bauer, M. Beker, S. Bigotta, S. Birindelli, *et al.*, 2010b, Astroparticle Physics **33**(3), 182 , ISSN 0927-6505.

Acernese, F., F. Antonucci, S. Aoudia, K. G. Arun, P. Astone, G. Ballardin, F. Barone, M. Barsuglia, T. S. Bauer, M. G. Beker, S. Bigotta, S. Birindelli, *et al.*, 2010, Astroparticle Physics **33**, 75.

Adhikari, R., 2004, *Sensitivity and Noise Analysis of 4 km Laser Interferometric Gravitational Wave Antennae*, Ph.D. thesis, Massachusetts Institute of Technology, URL http://hdl.handle.net/1721.1/28646.

Ageev, A., B. C. Palmer, A. D. Felice, S. D. Penn, and P. R. Saulson, 2004, Classical and Quantum Gravity **21**(16), 3887.

Ajith, P., M. Boyle, D. A. Brown, B. Brügmann, L. T. Buchman, L. Cadonati, M. Campanelli, T. Chu, Z. B. Etienne, S. Fairhurst, M. Hannam, J. Healy, *et al.*, 2012, Classical and Quantum Gravity **29**(12), 124001, URL http://stacks.iop.org/0264-9381/29/i=12/a=124001.

Aki, K., and P. G. Richards, 2009, *Quantitative Seismology, 2nd edition* (University Science Books).

Allen, B., 1988, Phys. Rev. D **37**, 2078, URL http://link.aps.org/doi/10.1103/PhysRevD.37.2078.

Allen, B., 1997, in *Relativistic Gravitation and Gravitational Radiation*, edited by J.-A. Marck & J.-P. Lasota, p. 373, eprint arXiv:gr-qc/9604033.

Allen, B., W. G. Anderson, P. R. Brady, D. A. Brown, and J. D. E. Creighton, 2012, Phys. Rev. D **85**, 122006, URL http://link.aps.org/doi/10.1103/PhysRevD.85.122006.

Ando, M., K. Ishidoshiro, K. Yamamoto, K. Yagi, W. Kokuyama, K. Tsubono, and A. Takamori, 2010a, Phys. Rev. Lett. **105**, 161101.

Ando, M., S. Kawamura, N. Seto, S. Sato, T. Nakamura, K. Tsubono, T. Takashima, I. Funaki, K. Numata, N. Kanda, T. Tanaka, K. Ioka, *et al.*, 2010b, Classical and Quantum Gravity **27**(8), 084010.

Ando, S., B. Baret, B. Bouhou, E. Chassande-Motting, A. Kouchner, L. Moscoso, V. Van Elewyck, I. Bartos, S. Marka, Z. Marka, A. Corsi, I. Di Palma, *et al.*, 2012, submitted to RMP (LIGO-P1100194).

Anholm, M., S. Ballmer, J. D. E. Creighton, L. R. Price, and X. Siemens, 2009, Phys. Rev. D **79**, 084030, URL http://link.aps.org/doi/10.1103/PhysRevD.79.084030.

Arai, K., R. Takahashi, D. Tatsumi, K. Izumi, Y. Wakabayashi, H. Ishizaki, M. Fukushima, T. Yamazaki, M.-K. Fujimoto, A. Takamori, K. Tsubono, R. DeSalvo, *et al.*, 2009, Classical and Quantum Gravity **26**(20), 204020.

Arai, K., and TAMA Collaboration, 2002, Classical and Quantum Gravity **19**, 1843.

Arain, M. A., and G. Mueller, 2008, Optics Express **16**(14), 10018.

Armstrong, J. W., 2006, Living Reviews in Relativity **9**(1), URL http://www.livingreviews.org/lrr-2006-1.

Armstrong, J. W., L. Iess, P. Tortora, and B. Bertotti, 2003, Astrophysical Journal .

Asmar, S. W., J. W. Armstrong, L. Iess, and P. Tortora, 2005, Radio Science **40**, RS2001.

Aso, Y., and A. Araya, 2012, Kamioka seismic data, personal communication.

Aston, S. M., M. A. Barton, A. S. Bell, N. Beveridge, B. Bland, A. J. Brummitt, G. Cagnoli, C. A. Cantley, L. Carbone, A. V. Cumming, L. Cunningham, R. M. Cutler, *et al.*, 2012, Classical and Quantum Gravity **29**(23), 235004, URL http://stacks.iop.org/0264-9381/29/i=23/a=235004.

Aufmuth, P., and K. Danzmann, 2005, New Journal of Physics **7**, 252.

Augst, S. J., and R. W. P. Drever, 2000, AIP Conference Proceedings **523**(1), 338, URL http://link.aip.org/link/?APC/523/338/1.

Ballardin, G., L. Bracci, S. Braccini, C. Bradaschia, C. Casciano, G. Calamai, R. Cavalieri, R. Cecchi, G. Cella, E. Cuoco, E. D'Ambrosio, V. Dattilo, *et al.*, 2001, Review of Scientific Instruments **72**(9), 3643.

Ballmer, S. W., 2006, *LIGO interferometer operating at design sensitivity with application to gravitational radiometry*, Ph.D. thesis, Massachusetts Institute of Technology, Massachusetts, USA.

Balser, M., and C. A. Wagner, 1960, Nature **188**, 638.

Barish, B., and R. Weiss, 1999, Physics Today **52**(10), 44.

Barkhausen, H., 1919, Phys. Zeitschrift **20**, 401.

Barsotti, L., 2006, *The control of the Virgo interferometer for gravitational wave detection*, Ph.D. thesis, University of Pisa.

Barsotti, L., M. Evans, and P. Fritschel, 2010, Classical and Quantum Gravity **27**(8), 084026, URL http://stacks.iop.org/0264-9381/27/i=8/a=084026.

Bass, M., and V. Mahajan, 2009, *Handbook of Optics: Geometrical and Physical Optics, Polarized Light, Components and Instruments*, v. 1 (McGraw-Hill), ISBN 9780071498890, URL http://books.google.com/books?id=xmDntwAACAAJ.

Bassiri, R., K. Evans, K. Borisenko, M. Fejer, J. Hough, I. MacLaren, I. Martin, R. Route, and S. Rowan, 2012, Acta Materialia (0), , ISSN 1359-6454, URL http://www.sciencedirect.com/science/article/pii/S1359645412007343.

Beccaria, M., M. Bernardini, S. Braccini, C. Bradaschia, A. Bozzi, C. Casciano, G. Cella, A. Ciampa, E. Cuoco, G. Curci, E. D'Ambrosio, V. Dattilo, *et al.*, 1998a, Classical and Quantum Gravity **15**(11), 3339.

Beccaria, M., M. Bernardini, S. Braccini, C. Bradaschia, A. Bozzi, C. Casciano, G. Cella, A. Ciampa, E. Cuoco, G. Curci, E. D'Ambrosio, V. Dattilo, *et al.*, 1998b, Classical and Quantum Gravity **15**(11), 3339, URL http://stacks.iop.org/0264-9381/15/i=11/a=004.

Beker, M. G., G. Cella, R. Desalvo, M. Doets, H. Grote, J. Harms, E. Hennes, V. Mandic, D. S. Rabeling, J. F. J. van den Brand, and C. M. van Leeuwen, 2011, General Relativity and Gravitation **43**, 623.

Belczynski, K., V. Kalogera, and T. Bulik, 2002, The Astrophysical Journal **572**, 407.

Bender, P. L., 2011, Phys. Rev. D **84**, 028101, URL http://link.aps.org/doi/10.1103/PhysRevD.84.028101.

Bender, P. L., 2011, General Relativity and Gravitation **44**, 337.

Bernard, W., and H. B. Callen, 1959, Rev. Mod. Phys. **31**, 1017, URL http://link.aps.org/doi/10.1103/RevModPhys.31.1017.

Bertotti, G., 1998, *Hysteresis in Magnetism: For Physicists, Materials Scientists, and Engineers*, Electromagnetism Series (Academic Press), ISBN 9780120932702, URL http://books.google.com/books?id=B7xZctzCPfgC.

Beyersdorf, P. T., R. L. Byer, and M. M. Fejer, 2000, AIP Conference Proceedings **523**(1), 200.

Bildsten, L., 1998, The Astrophysical Journal Letters **501**(1), L89.

Bittel, H., 1969, IEEE Transactions on Magnetics **5**, 359.

Blair, D., E. Howell, L. Ju, and C. Zhao, 2012, *Advanced Gravitational Wave Detectors* (Cambridge University Press), ISBN 9780521874298, URL http://books.google.com/books?id=mvVBkgQZrecC.

Bochner, B., 2003, General Relativity and Gravitation **35**, 1029, ISSN 0001-7701, 10.1023/A:1024016917669.

Borselli, M., T. J. Johnson, and O. Painter, 2006, Applied Physics Letters **88**(13), 131114.

Brady, P. R., T. Creighton, C. Cutler, and B. F. Schutz, 1998, Phys. Rev. D **57**, 2101.

Braginsky, V. B., 2008, Astronomy Letters **34**(8), 558.

Braginsky, V. B., M. L. Gorodetsky, F. Y. Khalili, and K. S. Thorne, 2000, Phys. Rev. D **61**, 044002.

Braginsky, V. B., and F. Y. Khalili, 1996, Rev. Mod. Phys. **68**, 1.

Braginsky, V. B., and F. Y. Khalili, 1999, *Quantum Measurement* (Cambridge University Press).

Braginsky, V. B., O. G. Ryazhskaya, and S. P. Vyatchanin, 2006, Physics Letters A **359**(2), 86.

Braginsky, V. B., S. E. Strigin, and S. P. Vyatchanin, 2001, Physics Letters A **287**, 331.

Braginsky, V. B., S. E. Strigin, and S. P. Vyatchanin, 2002, Physics Letters A **305**, 111.

Braginsky, V. B., and S. P. Vyatchanin, 2003, Phys. Lett. A **312**, 244.

Brooks, A. F., D. Hosken, J. Munch, P. J. Veitch, Z. Yan, C. Zhao, Y. Fan, L. Ju, D. Blair, P. Willems, B. Slagmolen, and J. Degallaix, 2009, Appl. Opt. **48**, 355.

Brown, B. L., A. P. Mills, and J. A. Tyson, 1982, Phys. Rev.

D **26**, 1209.
Buonanno, A., and Y. Chen, 2001, Phys. Rev. D **64**, 042006.
Buonanno, A., and Y. Chen, 2002, Phys. Rev. D **65**, 042001.
Cagnoli, G., L. Gammaitoni, J. Kovalik, and F. Marchesoni, 1999, Physics Letters A .
Cagnoli, G., J. Hough, D. DeBra, M. Fejer, E. Gustafson, S. Rowan, and V. Mitrofanov, 2000, Physics Letters A **272**(1-2), 39 , ISSN 0375-9601.
Cagnoli, G., and P. A. Willems, 2002, Phys. Rev. B **65**, 174111, URL http://link.aps.org/doi/10.1103/PhysRevB.65.174111.
Callen, H. B., and T. A. Welton, 1951, Phys. Rev. **83**, 34.
Camp, J. B., H. Yamamoto, S. E. Whitcomb, and D. E. McClelland, 2000, Journal of the Optical Society of America A **17**, 120.
Campbell, W. H., 1965, in *Report on Equatorial Aeronomy*, edited by F. de Mendonça, p. 495.
Caves, C. M., 1980, Phys. Rev. D **23**, 1693.
Caves, C. M., and B. L. Schumaker, 1985, Phys. Rev. A **31**, 3068 & 3093.
Cella, G., and A. Giazotto, 2011, Review of Scientific Instruments **82**(10), 101101 (pages 44).
Chakrabarty, D., E. H. Morgan, M. P. Muno, D. K. Galloway, R. Wijnands, M. van der Klis, and C. B. Markwardt, 2003, Nature **424**(6944), 42.
Chapline, G. F., J. Nuckolls, and L. L. Wood, 1974, Phys. Rev. D **10**, 1064.
Chelkowski, S., S. Hild, and A. Freise, 2009, Phys. Rev. D **79**, 122002.
Chen, Y., 2013, ArXiv e-prints eprint 1302.1924.
Chen, Y., S. L. Danilishin, F. Y. Khalili, and H. Müller-Ebhardt, 2010, General Relativity and Gravitation **43**(2), 671.
Chua, S. S. Y., M. S. Stefszky, C. M. Mow-Lowry, B. C. Buchler, S. Dwyer, D. A. Shaddock, P. K. Lam, and D. E. McClelland, 2011, Optics Letters **36**, 4680.
Cole, G. D., S. Groblacher, K. Gugler, S. Gigan, and M. Aspelmeyer, 2008, Applied Physics Letters **92**(26), 261108 (pages 3).
Collaboration, T. V., 2008, Appl. Opt. **47**(31), 5853, URL http://ao.osa.org/abstract.cfm?URI=ao-47-31-5853.
Collaboration, T. V., 2010, Appl. Opt. **49**(25), 4780, URL http://dx.doi.org/10.1364/ao.49.004780.
Corbitt, T., and N. Mavalvala, 2004, Journal of Optics B: Quantum and Semiclassical Optics **6**(8), S675.
Corbitt, T., D. Ottaway, E. Innerhofer, J. Pelc, and N. Mavalvala, 2006, Phys. Rev. A **74**, 021802, URL http://link.aps.org/doi/10.1103/PhysRevA.74.021802.
Cornish, N. J., and E. K. Porter, 2007, Phys. Rev. D **75**, 021301.
Creighton, T., 2008, Classical and Quantum Gravity **25**(12), 125011.
Cumming, A. V., A. S. Bell, L. Barsotti, M. A. Barton, G. Cagnoli, D. Cook, L. Cunningham, M. Evans, G. D. Hammond, G. M. Harry, A. Heptonstall, J. Hough, *et al.*, 2012, Classical and Quantum Gravity **29**(3), 035003, URL http://stacks.iop.org/0264-9381/29/i=3/a=035003.
Cutler, C., and J. Harms, 2006, Phys. Rev. D **73**, 042001.
Cutler, C., and D. E. Holz, 2009, Phys. Rev. D **80**, 104009, URL http://link.aps.org/doi/10.1103/PhysRevD.80.104009.
Cutler, C., and K. S. Thorne, 2002, ArXiv General Relativity and Quantum Cosmology e-prints eprint arXiv:gr-qc/0204090.
D'Ambrosio, E., R. O'Shaugnessy, K. Thorne, P. Willems, S. Strigin, and S. Vyatchanin, 2004, Classical and Quantum Gravity **21**(5), S867.
Danzmann, K., and A. Rüdiger, 2003, Classical and Quantum Gravity **20**(10), S1.
Daw, E. J., J. A. Giaime, D. Lormand, M. Lubiński, and J. Zweizig, 2004, Classical and Quantum Gravity **21**, 2255.
DECIGO, 2011, DECIGO homepage, URL http://tamago.mtk.nao.ac.jp/decigo/.
Demeester, P., I. Pollentier, P. D. Dobbelaere, C. Brys, and P. V. Daele, 1993, Semiconductor Science and Technology **8**(6), 1124, URL http://stacks.iop.org/0268-1242/8/i=6/a=021.
DeRosa, R., J. C. Driggers, D. Atkinson, H. Miao, V. Frolov, M. Landry, J. A. Giaime, and R. X. Adhikari, 2012, Classical and Quantum Gravity **29**(21), 215008, URL http://stacks.iop.org/0264-9381/29/i=21/a=215008.
Detweiler, S., 1979, The Astrophysical Journal **234**.
Dimopoulos, S., P. W. Graham, J. M. Hogan, M. A. Kasevich, and S. Rajendran, 2008, Phys. Rev. D **78**, 122002.
Dimopoulos, S., P. W. Graham, J. M. Hogan, M. A. Kasevich, and S. Rajendran, 2011, Phys. Rev. D **84**, 028102, URL http://link.aps.org/doi/10.1103/PhysRevD.84.028102.
Dooley, K., 2011, *Design and Performance of High Laser Power Interferometers for Gravitational-wave Detection*, Ph.D. thesis, University of Florida.
Douglass, D. H., R. Q. Gram, J. A. Tyson, and R. W. Lee, 1975, Phys. Rev. Lett. **35**, 480.
Drever, R. W. P., 1983, in *Lecture Notes in Physics*, volume 124 of *Berlin Springer Verlag*, pp. 321–338.
Drever, R. W. P., 1983, AIP Conference Proceedings **96**(1), 336.
Drever, R. W. P., 1991, in *The Detection of Gravitational Waves*, edited by D. G. Blair, p. 306.
Drever, R. W. P., 1996, in *Dark Matter in Cosmology Quantam Measurements Experimental Gravitation*, edited by R. Ansari, Y. Giraud-Heraud, and J. Tran Thanh Van, p. 375.
Drever, R. W. P., J. L. Hall, F. V. Kowalski, J. Hough, G. M. Ford, A. J. Munley, and H. Ward, 1983, Applied Physics B: Lasers and Optics **31**, 97.
Driggers, J., and J. Harms, 2011, *Results of Phase 1 Newtonian Noise Measurements at the LIGO Sites*, Technical Report T1100237, LIGO, https://dcc.ligo.org/cgi-bin/DocDB/ShowDocument?docid=60064.
Driggers, J. C., M. Evans, K. Pepper, and R. Adhikari, 2012a, Review of Scientific Instruments **83**(2), 024501.
Driggers, J. C., J. Harms, and R. X. Adhikari, 2012b, Phys. Rev. D **86**, 102001, URL http://link.aps.org/doi/10.1103/PhysRevD.86.102001.
Durin, G., and S. Zapperi, 2004, eprint arXiv:cond-mat/0404512 eprint arXiv:cond-mat/0404512.
Dwyer, S., 2012, Ph.D. thesis, Massachusetts Institute of Technology.
Einstein, A., 1916, Sitzungsberichte der Königlich Preußischen Akademie der Wissenschaften (Berlin) **33**, 688.
Einstein, A., 1918, Sitzungsberichte der Königlich Preußischen Akademie der Wissenschaften (Berlin) **8**, 154.
Einstein, A., and A. Engel, 1997, *The Collected Papers of Albert Einstein: The Berlin Years: Writings, 1914-1917*, The Collected Papers of Albert Einstein (Princeton University Press), ISBN 9780691017341, URL http://books.google.com/books?id=AfMclQEACAAJ.

Einstein @ Home, 2012, URL http://einstein.phys.uwm.edu/.

Einstein Telescope Science Team, 2011, Einstein gravitational wave Telescope conceptual design study, URL http://www.et-gw.eu/.

Estabrook, F. B., and H. D. Wahlquist, 1975, General Relativity and Gravitation **6**, 439.

Evans, K., R. Bassiri, I. Maclaren, S. Rowan, I. Martin, J. Hough, and K. Borisenko, 2012, in *Journal of Physics: Conference Series* (IOP Publishing), volume 371, p. 012058.

Evans, M., S. Ballmer, M. Fejer, P. Fritschel, G. Harry, and G. Ogin, 2008, Phys. Rev. D **78**, 102003.

Evans, M., L. Barsotti, and P. Fritschel, 2010, Physics Letters A **374**(4), 665 , ISSN 0375-9601.

Faller, J., P. Bender, J. Hall, D. Hils, R. Stebbins, and M. Vincent, 1989, Advances in Space Research **9**(9), 107 , ISSN 0273-1177.

Farmer, A. J., and E. S. Phinney, 2003, Monthly Notices of the Royal Astronomical Society **346**(4), 1197, ISSN 1365-2966.

Faye, G., S. Marsat, L. Blanchet, and B. R. Iyer, 2012, Classical and Quantum Gravity **29**(17), 175004, URL http://stacks.iop.org/0264-9381/29/i=17/a=175004.

Feynman, R. P., 1965, *Feynman lectures on physics. Volume 3: Quantum mechanics* (Addison-Wesley).

Flaminio, R., J. Franc, C. Michel, N. Morgado, L. Pinard, and B. Sassolas, 2010, Classical and Quantum Gravity **27**(8), 084030.

Flanagan, E. E., and K. S. Thorne, 1995, *Scattered-Light Noise for LIGO*, Technical Report, LIGO, https://dcc.ligo.org/cgi-bin/DocDB/ShowDocument?docid=28576.

Freise, A., and K. A. Strain, 2010, Living Reviews in Relativity **13**(1), URL http://www.livingreviews.org/lrr-2010-1.

Fricke, T., N. Smith-Lefebvre, R. Abbott, R. Adhikari, K. L. Dooley, M. Evans, P. Fritschel, V. Frolov, K. Kawabe, J. S. Kissel, and S. Waldman, 2012, Classical and Quantum Gravity eprint 1110.2815.

Fritschel, P., R. Bork, G. González, N. Mavalvala, D. Ouimette, H. Rong, D. Sigg, and M. Zucker, 2001, Appl. Opt. **40**(28), 4988, URL http://dx.doi.org/10.1364/AO.40.004988.

Fritschel, P., D. Shoemaker, and R. Weiss, 1992, Appl. Opt **31**(10), 1412.

Gaidarzhy, A., M. Imboden, P. Mohanty, J. Rankin, and B. W. Sheldon, 2007, Applied Physics Letters **91**(20), 203503.

Giaime, J., P. Saha, D. Shoemaker, and L. Sievers, 1996, Review of Scientific Instruments **67**(1), 208.

Giaime, J. A., E. J. Daw, M. Weitz, R. Adhikari, P. Fritschel, R. Abbott, R. Bork, and J. Heefner, 2003, Review of Scientific Instruments **74**(1), 218, URL http://link.aip.org/link/?RSI/74/218/1.

Giazotto, A., 1989, Physics Reports **182**(6), 365.

Giazotto, A., 1998, Physics Letters A **245**(3–4), 203 , ISSN 0375-9601, URL http://www.sciencedirect.com/science/article/pii/S0375960198004113.

Giazotto, A., 2011, Physics Letters A .

Gillespie, A., and F. Raab, 1995, Phys. Rev. D **52**, 577.

Goda, K., O. Miyakawa, E. E. Mikhailov, S. Saraf, R. Adhikari, K. McKenzie, R. Ward, S. Vass, A. J. Weinstein, and N. Mavalvala, 2008, Nature Physics **4**, 472.

González, G., 2000, Classical and Quantum Gravity .

González, G. I., and P. R. Saulson, 1994, The Journal of the Acoustical Society of America **96**(1), 207.

Granata, M., M. Barsuglia, R. Flaminio, A. Freise, S. Hild, and J. Marque, 2010a, Journal of Physics: Conference Series **228**(1), 012016.

Granata, M., C. Buy, R. Ward, and M. Barsuglia, 2010b, Phys. Rev. Lett. **105**, 231102.

Gras, S., D. G. Blair, and C. Zhao, 2009, Classical and Quantum Gravity **26**(13), 135012, URL http://stacks.iop.org/0264-9381/26/i=13/a=135012.

Gretarsson, A., and G. Harry, 1999, Review of scientific instruments **70**(10), 4081.

Gretarsson, A. M., E. D'Ambrosio, V. Frolov, B. O'Reilly, and P. K. Fritschel, 2007, J. Opt. Soc. Am. B **24**(11), 2821, URL http://dx.doi.org/10.1364/JOSAB.24.002821.

Gretarsson, A. M., G. M. Harry, S. D. Penn, P. R. Saulson, W. J. Startin, S. Rowan, G. Cagnoli, and J. Hough, 2000, Physics Letters A **270**, 108.

Gréverie, C., A. Brillet, C. N. Man, W. Chaibi, J. P. Coulon, and K. Feliksik, 2010, in *Conference on Lasers and Electro-Optics* (Optical Society of America), p. JTuD36, URL http://www.opticsinfobase.org/abstract.cfm?URI=CLEO-2010-JTuD36.

Grote, H., 2003, *Making it Work: Second Generation Interferometry in GEO 600!*, Ph.D. thesis, Universität Hannover.

Grote, H., 2008, Classical and Quantum Gravity **25**(11), 114043.

Grote, H., 2010, Classical and Quantum Gravity **27**(8), 084003.

Grote, H., G. Heinzel, A. Freise, S. Gossler, and B. Willke, 2002, Classical and Quantum Gravity .

Hammond, G. D., A. V. Cumming, J. Hough, R. Kumar, K. Tokmakov, S. Reid, and S. Rowan, 2012, Classical and Quantum Gravity **29**(12), 124009.

Hammond, G. D., A. Pulido-Paton, C. C. Speake, and C. Trenkel, 2004, Review of Scientific Instruments **75**, 955.

Hardham, C., B. Abbott, R. Abbott, G. Allen, R. Bork, C. Campbell, K. Carter, D. Coyne, D. DeBra, T. Evans, *et al.*, 2004, in *in Proceedings of ASPE Spring Topical Meeting on Control of Precision Systems*, pp. 127–132.

Harms, J., Y. Chen, S. Chelkowski, and A. Franzen, 2003, Physical Review D .

Harry, G., T. Bodiya, and R. DeSalvo, 2012, *Optical Coatings and Thermal Noise in Precision Measurement*, Optical Coatings and Thermal Noise in Precision Measurement (Cambridge University Press), ISBN 9781107003385, URL http://books.google.com/books?id=770n4QLmBrMC.

Harry, G. M., 2010, Classical and Quantum Gravity **27**(8), 084006.

Harry, G. M., M. R. Abernathy, A. E. Becerra-Toledo, H. Armandula, E. Black, K. Dooley, M. Eichenfield, C. Nwabugwu, A. Villar, D. R. M. Crooks, G. Cagnoli, J. Hough, *et al.*, 2007, Classical and Quantum Gravity **24**(2), 405.

Harry, G. M., H. Armandula, E. Black, D. R. M. Crooks, G. Cagnoli, J. Hough, P. Murray, S. Reid, S. Rowan, P. Sneddon, M. M. Fejer, R. Route, *et al.*, 2006, Appl. Opt. **45**(7), 1569.

Harry, G. M., A. M. Gretarsson, P. R. Saulson, S. E. Kittelberger, S. D. Penn, W. J. Startin, S. Rowan, M. M. Fejer, D. R. M. Crooks, G. Cagnoli, J. Hough, and N. Nakagawa, 2002, Classical and Quantum Gravity **19**(5), 897.

Hawking, S., and W. Israel (eds.), 1989, *Three Hun-*

dred Years of Gravitation, Philosophiae Naturalis, Principia Mathematica (Cambridge University Press), ISBN 9780521379762.
Haykin, S., 2002, *Adaptive Filter Theory*, Prentice-Hall information and system sciences series (Prentice Hall), ISBN 9780130901262.
Hebard, A. F., 1973, Review of Scientific Instruments **44**, 425.
Heinzel, G., K. A. Strain, J. Mizuno, K. D. Skeldon, B. Willke, W. Winkler, R. Schilling, A. Rüdiger, and K. Danzmann, 1998, Phys. Rev. Lett. **81**, 5493.
Hellings, R. W., and G. S. Downs, 1982, The Astrophysical Journal **265**.
Hello, P., and J. Vinet, 1990, Journal de Physique **51**(12), 1267.
Hello, P., and J.-Y. Vinet, 1993, Physics Letters A **178**(5), 351.
Hensley, J. M., A. Peters, and S. Chu, 1999, Review of Scientific Instruments **70**(6), 2735.
Heptonstall, A., M. Barton, C. Cantley, A. Cumming, G. Cagnoli, J. Hough, R. Jones, R. Kumar, I. Martin, S. Rowan, *et al.*, 2010, Classical and Quantum Gravity **27**(3), 035013.
Herriott, D. R., and H. J. Schulte, 1965, Appl. Opt. **4**(8), 883.
Hewish, A., S. J. Bell, J. D. H. Pilkington, P. F. Scott, and R. A. Collins, 1968, Nature **217**(5130), 709.
Hild, S., H. Lück, W. Winkler, K. Strain, H. Grote, J. Smith, M. Malec, M. Hewitson, B. Willke, J. Hough, and K. Danzmann, 2006, Appl. Opt. **45**, 7269.
Hirose, E., K. Kawabe, D. Sigg, R. Adhikari, and P. R. Saulson, 2010, Appl. Opt. **49**(18), 3474.
Hohensee, M., S.-Y. Lan, R. Houtz, C. Chan, B. Estey, G. Kim, P.-C. Kuan, and H. Müller, 2011, General Relativity and Gravitation **43**, 1905, ISSN 0001-7701, 10.1007/s10714-010-1118-x.
Hong, T., J. Miller, H. Yamamoto, Y. Chen, and R. Adhikari, 2011, Phys. Rev. D **84**, 102001.
Hong, T., H. Yang, E. Gustafson, R. Adhikari, and Y. Chen, 2012, arXiv preprint arXiv:1207.6145 .
Hu, W., and S. Dodelson, 2002, Annual Review of Astronomy and Astrophysics **40**, 171.
Huang, Y., J. Benesty, and J. Chen, 2006, *Acoustic MIMO signal processing*, Signals and communication technology (Springer), ISBN 9783540376309.
Hughes, S. A., and K. S. Thorne, 1998, Phys. Rev. D **58**, 122002.
Ipser, J. R., 1971, Astrophys. J. **166**, 175.
Ishidoshiro, K., M. Ando, A. Takamori, H. Takahashi, K. Okada, N. Matsumoto, W. Kokuyama, N. Kanda, Y. Aso, and K. Tsubono, 2011, Phys. Rev. Lett. **106**, 161101.
Jayawant, B. V., 1981, Reports on Progress in Physics **44**(4), 411, URL http://stacks.iop.org/0034-4885/44/i=4/a=002.
Ju, L., D. G. Blair, and C. Zhao, 2000, Reports on Progress in Physics **63**(9), 1317.
Ju, L., D. G. Blair, C. Zhao, S. Gras, Z. Zhang, P. Barriga, H. Miao, Y. Fan, and L. Merrill, 2009, Classical and Quantum Gravity **26**(1), 015002, URL http://stacks.iop.org/0264-9381/26/i=1/a=015002.
KAGRA, 2011, KAGRA home page, URL http://gwcenter.icrr.u-tokyo.ac.jp/en/.
Khalili, F. Y., 2002, Phys. Lett. A **298**, 308.
Khalili, F. Y., 2007, Phys. Rev. D **76**, 102002.
Kimble, H. J., Y. Levin, A. B. Matsko, K. S. Thorne, and S. P. Vyatchanin, 2001, Phys. Rev. D **65**, 022002.
Kippenberg, T. J., H. Rokhsari, T. Carmon, A. Scherer, and K. J. Vahala, 2005, Phys. Rev. Lett. **95**, 033901, URL http://link.aps.org/doi/10.1103/PhysRevLett.95.033901.
Knispel, B., P. Lazarus, B. Allen, D. Anderson, C. Aulbert, N. D. R. Bhat, O. Bock, S. Bogdanov, A. Brazier, F. Camilo, S. Chatterjee, J. M. Cordes, *et al.*, 2011, The Astrophysical Journal Letters **732**(1), L1, URL http://stacks.iop.org/2041-8205/732/i=1/a=L1.
Kondratiev, N. M., A. G. Gurkovsky, and M. L. Gorodetsky, 2011, Phys. Rev. D **84**, 022001.
Kovalik, J., and P. R. Saulson, 1993, Review of Scientific Instruments **64**(10), 2942, URL http://link.aip.org/link/?RSI/64/2942/1.
Królak, A., M. Tinto, and M. Vallisneri, 2004, Phys. Rev. D **70**, 022003.
Kubo, R., 1966, Reports on Progress in Physics **29**, 255.
Kwee, P., B. Willke, and K. Danzmann, 2009, Opt. Lett. **34**(19), 2912, URL http://ol.osa.org/abstract.cfm?URI=ol-34-19-2912.
Lada, C. J., 2006, The Astrophysical Journal Letters **640**(1), L63, URL http://stacks.iop.org/1538-4357/640/i=1/a=L63.
Lantz, B., R. Schofield, B. O'Reilly, D. E. Clark, and D. DeBra, 2009, Bulletin of the Seismological Society of America **99**(2B), 980.
Lawrence, R., D. Ottaway, M. Zucker, and P. Fritschel, 2004, Optics Letters **29**(22), 2635.
Leibrandt, D. R., J. C. Bergquist, and T. Rosenband, 2013, ArXiv e-prints eprint 1301.0022.
Levin, Y., 1998, Phys. Rev. D **57**, 659, URL http://link.aps.org/doi/10.1103/PhysRevD.57.659.
LIGO, 2011, URL https://www.advancedligo.mit.edu/.
LIGO Scientific Collaboration, J. Abadie, B. P. Abbott, R. Abbott, T. D. Abbott, M. Abernathy, C. Adams, R. Adhikari, C. Affeldt, B. Allen, and et al., 2011, Nature Physics **7**, 962.
Lin, A. C., J. S. Harris, and M. M. Fejer, 2011, Journal of Vacuum Science Technology B: Microelectronics and Nanometer Structures **29**(3), 030000.
Liu, Y. T., and L. Lindblom, 2001, Monthly Notices of the Royal Astronomical Society **324**, 1063.
Logan, J. E., J. Hough, and N. A. Robertson, 1993, Physics Letters A .
Lorén-Aguilar, P., J. Guerrero, J. Isern, J. A. Lobo, and E. García-Berro, 2005, Monthly Notices of the Royal Astronomical Society **356**, 627.
Lorimer, D. R., 2008, Living Reviews in Relativity **11**(8).
Loudon, R., 1981, Phys. Rev. Lett. **47**, 815.
Lück, H., C. Affeldt, J. Degallaix, A. Freise, H. Grote, M. Hewitson, S. Hild, J. Leong, M. Prijatelj, K. A. Strain, B. Willke, H. Wittel, *et al.*, 2010, Journal of Physics: Conference Series **228**(1), 012012+, ISSN 1742-6596, URL http://dx.doi.org/10.1088/1742-6596/228/1/012012.
Lück, H., J. Degallaix, H. Grote, M. Hewitson, S. Hild, B. Willke, and K. Danzmann, 2008, Journal of Optics A: Pure and Applied Optics **10**(8), 085004.
Lück, H., A. Freise, S. Goßler, S. Hild, K. Kawabe, and K. Danzmann, 2004, Classical and Quantum Gravity **21**(5), 985.
Lück, H., M. Hewitson, P. Ajith, B. Allen, P. Aufmuth, C. Aulbert, S. Babak, R. Balasubramanian, B. W. Barr, S. Berukoff, A. Bunkowski, G. Cagnoli, *et al.*, 2006, Clas-

sical and Quantum Gravity **23**, 71.
Mandic, V., and A. Buonanno, 2006, Phys. Rev. D **73**, 063008, URL http://link.aps.org/doi/10.1103/PhysRevD.73.063008.
Márka, S., A. Takamori, M. Ando, A. Bertolini, G. Cella, R. DeSalvo, M. Fukushima, Y. Iida, F. Jacquier, S. Kawamura, Y. Nishi, K. Numata, *et al.*, 2002, Classical and Quantum Gravity **19**(7), 1605.
Mavalvala, N., D. Shoemaker, D. Sigg, M. Zucker, and et al, 1998, Appl. Opt .
McClelland, D. E., N. Mavalvala, Y. Chen, and R. Schnabel, 2011, Laser & Photonics Reviews **5**(5), 677.
McClelland, D. E., C. M. Savage, A. J. Tridgell, and R. Mavaddat, 1993, Phys. Rev. D **48**, 5475, URL http://link.aps.org/doi/10.1103/PhysRevD.48.5475.
Mckenzie, K., 2008, *Squeezing in the Audio Gravitational Wave Detection Band*, Ph.D. thesis, Australian National University.
McKenzie, K., N. Grosse, W. P. Bowen, S. E. Whitcomb, M. B. Gray, D. E. McClelland, and P. K. Lam, 2004, Phys. Rev. Lett. **93**, 161105, URL http://link.aps.org/doi/10.1103/PhysRevLett.93.161105.
Meers, B. J., 1988, Phys. Rev. D **38**, 2317, URL http://link.aps.org/doi/10.1103/PhysRevD.38.2317.
Melchior, P., 1983, *The tides of the planet earth /2nd edition/*.
Miao, H., Y. Chen, and R. Adhikari, 2013, Comparison of quantum noise for optical configurations of laser-interferometric gravitational-wave detectors, in prep.
Miller, J., M. Evans, L. Barsotti, P. Fritschel, M. MacInnis, R. Mittleman, B. Shapiro, J. Soto, and C. Torrie, 2011, Physics Letters A **375**(3), 788 , ISSN 0375-9601, URL http://www.sciencedirect.com/science/article/pii/S0375960110015719.
Miller, J., P. Willems, H. Yamamoto, J. Agresti, and R. DeSalvo, 2008, Classical and Quantum Gravity **25**(23), 235016.
Misner, C. W., K. S. Thorne, and J. A. Wheeler, 1973, *Gravitation* (Freeman).
Mitrofanov, V., L. Prokhorov, K. Tokmakov, and P. Willems, 2004, Classical and Quantum Gravity **21**, 1083.
Miyakawa, O., R. Ward, R. Adhikari, M. Evans, B. Abbott, R. Bork, D. Busby, J. Heefner, A. Ivanov, M. Smith, R. Taylor, S. Vass, *et al.*, 2006, Phys. Rev. D **74**, 022001, URL http://link.aps.org/doi/10.1103/PhysRevD.74.022001.
Mizuno, J., 1995, *Comparison of optical configurations for laser-interferometric gravitational-wave detectors*, Ph.D. thesis, Universität Hannover and Max-Planck-Institut für Quantenoptik, Garching.
Mizuno, J., K. A. Strain, P. G. Nelson, J. M. Chen, R. Schilling, A. Rüdiger, W. Winkler, and K. Danzmann, 1993, Physics Letters A **175**, 273.
Morrison, E., B. Meers, D. Robertson, and H. Ward, 1994a, Applied Optics .
Morrison, E., B. J. Meers, D. I. Robertson, and H. Ward, 1994b, Applied Optics **33**(22), 5041, URL http://ao.osa.org/abstract.cfm?URI=ao-33-22-5041.
Mueller, G., Q. Shu, R. Adhikari, D. Tanner, and D. Reitze, 2000, Optics Letters .
Nawrodt, R., C. Schwarz, S. Kroker, I. W. Martin, F. Brückner, L. Cunningham, V. Große, A. Grib, D. Heinert, J. Hough, T. Käsebier, E. B. Kley, *et al.*, 2010, ArXiv e-prints eprint 1003.2893.
Newell, D. B., S. J. Richman, P. G. Nelson, R. T. Stebbins, P. L. Bender, J. E. Faller, and J. Mason, 1997, Review of Scientific Instruments **68**(8), 3211.
NGO, 2013, *Yellow Book*, Technical Report, NGO, URL http://elisa-ngo.org/publications/publications-yellow-book.
Ott, C. D., 2009, Classical and Quantum Gravity **26**(6), 063001, URL http://stacks.iop.org/0264-9381/26/i=6/a=063001.
Ottaway, D., J. Betzwieser, S. Ballmer, and S. Waldman, 2006, Optics . . . .
Ottaway, D. J., P. Fritschel, and S. J. Waldman, 2012, Opt. Express **20**(8), 8329, URL http://www.opticsexpress.org/abstract.cfm?URI=oe-20-8-8329.
Owen, B. J., 2005, Phys. Rev. Lett. **95**, 211101, URL http://link.aps.org/doi/10.1103/PhysRevLett.95.211101.
Owen, B. J., 2006, Classical and Quantum Gravity **23**, 1.
Pan, Y., 2006, ArXiv General Relativity and Quantum Cosmology e-prints eprint arXiv:gr-qc/0608128.
Peebles, P. J. E., 1993, *Principles of Physical Cosmology*, Princeton series in physics (Princeton University Press), ISBN 9780691019338, URL http://books.google.com/books?id=AmlEt6TJ6jAC.
Penn, S. D., A. Ageev, D. Busby, G. M. Harry, A. M. Gretarsson, K. Numata, and P. Willems, 2006, Physics Letters A **352**(1â“2), 3 , ISSN 0375-9601, URL http://www.sciencedirect.com/science/article/pii/S0375960105017846.
Penn, S. D., P. H. Sneddon, H. Armandula, J. C. Betzwieser, G. Cagnoli, J. Camp, D. R. M. Crooks, M. M. Fejer, A. M. Gretarsson, G. M. Harry, J. Hough, S. E. Kittelberger, *et al.*, 2003, Classical and Quantum Gravity **20**(13), 2917.
Peterson, J., 1993, Open-file report U. S. Geological Survey **93-322**.
Phillips, W. A., 1987, Reports on Progress in Physics **50**(12), 1657, URL http://stacks.iop.org/0034-4885/50/i=12/a=003.
Phinney, E. S., 1991, Astrophysical Journal Letters **380**, L17.
Phinney, E. S., 2003, NASA Mission Concept Study .
Pitkin, M., S. Reid, S. Rowan, and J. Hough, 2011, Living Reviews in Relativity **14**(5).
Plissi, M. V., K. A. Strain, C. I. Torrie, N. A. Robertson, S. Killbourn, S. Rowan, S. M. Twyford, H. Ward, K. D. Skeldon, and J. Hough, 1998, Review of Scientific Instruments **69**(8), 3055, URL http://link.aip.org/link/?RSI/69/3055/1.
Poenaru, D., and W. Greiner, 1997, *Experimental techniques in nuclear physics* (Walter de Gruyter), ISBN 9783110144673, URL http://books.google.com/books?id=7yq7ZV2G5D8C.
Pohl, R. O., X. Liu, and E. Thompson, 2002, Rev. Mod. Phys. **74**, 991.
Pollack, S. E., M. D. Turner, S. Schlamminger, C. A. Hagedorn, and J. H. Gundlach, 2010, Phys. Rev. D **81**, 021101, URL http://link.aps.org/doi/10.1103/PhysRevD.81.021101.
Ponslet, E. R., and W. O. Miller, 1998, in *Society of Photo-Optical Instrumentation Engineers (SPIE) Conference Series*, edited by L. P. Davis, volume 3327, pp. 432–443.
Prince, T., and the LISA Science Team, 2009, LISA: Probing the universe with gravitational waves.
Prince, T. A., M. Tinto, S. L. Larson, and J. W. Armstrong, 2002, Phys. Rev.D **66**, 122002.
Punturo, M., M. Abernathy, F. Acernese, B. Allen, N. Andersson, K. Arun, F. Barone, B. Barr, M. Barsuglia, M. Beker,

N. Beveridge, S. Birindelli, *et al.*, 2010, Classical and Quantum Gravity **27**(8), 084007.
Purdue, P., and Y. Chen, 2002, Phys. Rev. D **66**(12), 122004.
Regehr, M. W., 1995, Thesis (Ph.D.) - California Institute of Technology , 3.
Rehbein, H., H. Müller-Ebhardt, K. Somiya, S. L. Danilishin, R. Schnabel, K. Danzmann, and Y. Chen, 2008, Phys. Rev. D **78**, 062003, URL http://link.aps.org/doi/10.1103/PhysRevD.78.062003.
Rehbein, H., H. Müller-Ebhardt, K. Somiya, C. Li, R. Schnabel, K. Danzmann, and Y. Chen, 2007, Phys. Rev. D **76**, 062002, URL http://link.aps.org/doi/10.1103/PhysRevD.76.062002.
Rempe, G., R. J. Thompson, H. J. Kimble, and R. Lalezari, 1992, Optics Letters **17**, 363.
Ringler, A., and C. Hutt, 2010, Seismological Research Letters **81**(6), 972.
Robertson, N. A., G. Cagnoli, D. R. M. Crooks, E. Elliffe, J. E. Faller, P. Fritschel, S. Goßler, A. Grant, A. Heptonstall, J. Hough, H. Lück, R. Mittleman, *et al.*, 2002, Classical and Quantum Gravity **19**, 4043.
Rocchi, A., E. Coccia, V. Fafone, V. Malvezzi, Y. Minenkov, and L. Sperandio, 2012, Journal of Physics: Conference Series **363**(1), 2016.
Romero, F., and H. Dehnen, 1981, Zeitschrift Naturforschung Teil A **36**, 948.
Rowan, S., J. Hough, and D. R. M. Crooks, 2005, Physics Letters A **347**, 25.
Rubakov, V. A., M. V. Sazhin, and A. V. Veryaskin, 1982, Physics Letters B **115**, 189.
Saccorotti, G., D. Piccinini, L. Cauchie, and I. Fiori, 2011, Bulletin of the Seismological Society of America **101**(2), 568.
Sathyaprakash, B., M. Abernathy, F. Acernese, P. Ajith, B. Allen, P. Amaro-Seoane, N. Andersson, S. Aoudia, K. Arun, P. Astone, B. Krishnan, L. Barack, *et al.*, 2012, Classical and Quantum Gravity **29**(12), 124013.
Sathyaprakash, B., and B. F. Schutz, 2009, Living Reviews in Relativity **12**(2), URL http://www.livingreviews.org/lrr-2009-2.
Sato, S., S. Kawamura, M. Ando, T. Nakamura, K. Tsubono, A. Araya, I. Funaki, K. Ioka, N. Kanda, S. Moriwaki, M. Musha, K. Nakazawa, *et al.*, 2009, Journal of Physics: Conference Series **154**(1), 012040, URL http://stacks.iop.org/1742-6596/154/i=1/a=012040.
Sato, S., S. Miyoki, M. Ohashi, M.-K. Fujimoto, T. Yamazaki, M. Fukushima, A. Ueda, K.-I. Ueda, K. Watanabe, K. Nakamura, K. Etoh, N. Kitajima, *et al.*, 1999, Appl. Opt. **38**, 2880.
Saulson, P. R., 1984, Phys. Rev. D **30**, 732.
Saulson, P. R., 1990, Phys. Rev. D **42**, 2437.
Saulson, P. R., 1994, *Fundamentals of Interferometric Gravitational Wave Detectors* (World Scientific).
Sayed, A. H., 2003, *Fundamentals of Adaptive Filtering* (John Wiley & Sons).
Sazhin, M. V., 1978, Soviet Astronomy **22**.
Scheel, M. A., M. Boyle, T. Chu, L. E. Kidder, K. D. Matthews, and H. P. Pfeiffer, 2009, Phys. Rev. D **79**, 024003, URL http://link.aps.org/doi/10.1103/PhysRevD.79.024003.
Schilling, R., L. Schnupp, W. Winkler, H. Billing, K. Maischberger, and A. Rudiger, 1981, Journal of Physics E: Scientific Instruments **14**(1), 65, URL http://stacks.iop.org/0022-3735/14/i=1/a=018.
Schnabel, R., N. Mavalvala, D. E. McClelland, and P. K. Lam, 2010, Nature Communications **1**, 121.
Schnupp, L., W. Winkler, K. Maischberger, A. Rudiger, and R. Schilling, 1985, Journal of Physics E: Scientific Instruments **18**(6), 482.
Schofield, R., 2010, personal communication.
Shoemaker, D., R. Schilling, L. Schnupp, W. Winkler, K. Maischberger, and A. Rüdiger, 1988, Phys. Rev. D **38**, 423.
Sidles, J. A., and D. Sigg, 2006, Physics Letters A **354**, 167.
Siegman, A., 1986, *Lasers* (University Science Books), ISBN 9780935702118.
Smith-Lefebvre, N., S. Ballmer, M. Evans, S. Waldman, K. Kawabe, V. Frolov, and N. Mavalvala, 2011, Opt. Lett. **36**(22), 4365, URL http://ol.osa.org/abstract.cfm?URI=ol-36-22-4365.
Somiya, K., 2011, ArXiv e-prints eprint 1111.7185.
Starobinskii, A. A., 1979, JETP Letters **30**, 719.
Stefszky, M. S., C. M. Mow-Lowry, S. S. Y Chua, D. A. Shaddock, B. C. Buchler, H. Vahlbruch, A. Khalaidovski, R. Schnabel, P. K. Lam, and D. E. McClelland, 2012, Classical and Quantum Gravity **29**(14), 145015.
Strain, K. A., 2012, personal communication.
Strain, K. A., K. Danzmann, J. Mizuno, P. G. Nelson, A. Rüdiger, R. Schilling, and W. Winkler, 1994, Physics Letters A **194**(1), 124.
Strain, K. A., G. Müller, T. Delker, D. H. Reitze, D. B. Tanner, J. E. Mason, P. A. Willems, D. A. Shaddock, M. B. Gray, C. Mow-Lowry, and D. E. McClelland, 2003, Applied Optics **42**, 1244.
Strigin, S. E., and S. P. Vyatchanin, 2007, Physics Letters A **365**, 10.
Sun, K.-X., B. Allard, S. Buchman, S. Williams, and R. L. Byer, 2006, Classical and Quantum Gravity **23**, 141.
Sun, K.-X., M. M. Fejer, E. Gustafson, and R. L. Byer, 1996, Phys. Rev. Lett. **76**, 3053.
Sykora, D. M., and P. de Groot, 2011, in *Society of Photo-Optical Instrumentation Engineers (SPIE) Conference Series*, volume 8126 of *Society of Photo-Optical Instrumentation Engineers (SPIE) Conference Series*.
Szilágyi, B., L. Lindblom, and M. A. Scheel, 2009, Phys. Rev. D **80**(12), 124010.
Takahashi, R., 2012, personal communication.
Takahashi, R., K. Arai, D. Tatsumi, M. Fukushima, T. Yamazaki, M.-K. Fujimoto, K. Agatsuma, Y. Arase, N. Nakagawa, A. Takamori, K. Tsubono, R. DeSalvo, *et al.*, 2008, Classical and Quantum Gravity **25**(11), 114036.
Takahashi, R., Y. Saito, M. Fukushima, M. Ando, K. Arai, D. Tatsumi, G. Heinzel, S. Kawamura, T. Yamazaki, and S. Moriwaki, 2002, Journal of Vacuum Science and Technology A: Vacuum, Surfaces, and Films .
Tarallo, M. G., J. Miller, J. Agresti, E. D'Ambrosio, R. DeSalvo, D. Forest, B. Lagrange, J. M. Mackowsky, C. Michel, J. L. Montorio, N. Morgado, L. Pinard, *et al.*, 2007, Appl. Opt. **46**(26), 6648.
Tatsumi, D., 2008, J. Phys. Conf. **120**, 032011.
Tatsumi, D., K. Arai, and TAMA Collaboration, 2006, Journal of Physics Conference Series **32**, 94.
Taylor, J. H., L. A. Fowler, and P. M. McCulloch, 1979, Nature **277**, 437.
The Virgo Collaboration, 2009, VIR 027A 09 .
The Virgo Collaboration, 2012, *Advanced Virgo Technical Design Report*, Technical Report, URL https://tds.ego-gw.it/ql/?c=8940.

Thorne, K. S., 1989, *Light Scattering and Proposed Baffle Configuration for the LIGO*, LIGO Technical Report, Caltech, http://www.ligo.caltech.edu/docs/T/T890017-00.pdf.
Thorne, K. S., and C. J. Winstein, 1999, Phys. Rev. D **60**, 082001.
Thorpe, M. J., D. R. Leibrandt, T. M. Fortier, and T. Rosenband, 2010, Opt. Express **18**(18), 18744.
Tomaru, T., T. Suzuki, T. Uchiyama, A. Yamamoto, T. Shintomi, C. T. Taylor, K. Yamamoto, S. Miyoki, M. Ohashi, and K. Kuroda, 2002, Physics Letters A **301**, 215.
Turner, M., 1997, Physical Review D **55**(2), R435.
Tyson, J. A., and R. P. Giffard, 1978, Annual Review of Astronomy and Astrophysics **16**, 521.
Uehara, N., A. Ueda, K. Ueda, H. Sekiguchi, T. Mitake, K. Nakamura, N. Kitajima, and I. Kataoka, 1995, Optics letters **20**(6), 530.
Ugolini, D., M. Girard, G. M. Harry, and V. P. Mitrofanov, 2008, Physics Letters A **372**, 5741.
Ushomirsky, G., C. Cutler, and L. Bildsten, 2000, Monthly Notices of the Royal Astronomical Society **319**, 902.
Vahlbruch, H., S. Chelkowski, B. Hage, A. Franzen, K. Danzmann, and R. Schnabel, 2006, Phys. Rev. Lett. **97**, 011101, URL http://link.aps.org/doi/10.1103/PhysRevLett.97.011101.
Van Haasteren, R., Y. Levin, P. McDonald, and T. Lu, 2009, Monthly Notices of the Royal Astronomical Society **395**(2), 1005, ISSN 1365-2966, URL http://dx.doi.org/10.1111/j.1365-2966.2009.14590.x.
Varvella, M., E. Calloni, L. D. Fiore, L. Milano, and N. Arnaud, 2004, Astroparticle Physics **21**(3), 325 , ISSN 0927-6505, URL http://www.sciencedirect.com/science/article/pii/S0927650504000180.
de Vine, G., B. Ware, K. McKenzie, R. E. Spero, W. M. Klipstein, and D. A. Shaddock, 2010, Phys. Rev. Lett. **104**, 211103, URL http://link.aps.org/doi/10.1103/PhysRevLett.104.211103.
Vinet, J.-Y., 2010, Phys. Rev. D **82**, 042003.
Vinet, J.-Y., V. Brisson, and S. Braccini, 1996, Phys. Rev. D **54**, 1276.
Virgo, 2011, URL https://wwwcascina.virgo.infn.it/advirgo/.
Volland, H., 1995, *Handbook of Atmospheric Electrodynamics*, volume 1 of *Handbook of Atmospheric Electrodynamics* (CRC Press), ISBN 9780849386473.
Vyatchanin, S. P., and A. B. Matsko, 1996, JETP **82**, 1007.
Wahlquist, H., 1987, Gen. Rel. Gravitation **19**, 1101.
Walsh, C. J., A. J. Leistner, and B. F. Oreb, 1999, Appl. Opt. **38**(22), 4790, URL http://ao.osa.org/abstract.cfm?URI=ao-38-22-4790.
Webb, S., 1992, The Journal of the Acoustical Society of America **92**, 2141.
Weber, J., 1960, Phys. Rev. **117**, 306.
Weber, J., 1970, Phys. Rev. Lett. **24**, 276.
Weinberg, S., 2004, Phys. Rev. D **69**(2), 023503.
Weiss, R., 1972, *Electromagnetically Coupled Broadband Gravitational Antenna*, Technical Report, Massachusetts Institute of Technology, URL https://dcc.ligo.org/cgi-bin/DocDB/ShowDocument?docid=38618.
Weiss, R., 1999, Rev. Mod. Phys. **71**, S187.
Wenzel, 2012, URL http://www.wenzel.com/oscillators.htm.
Willemenot, E., and P. Touboul, 2000, Review of Scientific Instruments **71**(1), 310, URL http://link.aip.org/link/?RSI/71/310/1.
Willke, B., K. Danzmann, M. Frede, P. King, D. Kracht, P. Kwee, O. Puncken, R. L. Savage, Jr., B. Schulz, F. Seifert, C. Veltkamp, S. Wagner, *et al.*, 2008, Classical and Quantum Gravity **25**(11), 114040.
Winkler, W., K. Danzmann, A. Rüdiger, and R. Schilling, 1991, Phys. Rev. A **44**, 7022.
Winkler, W., R. Schilling, K. Danzmann, J. Mizuno, A. Rüdiger, and K. A. Strain, 1994, Appl. Opt. **33**(31), 7547, URL http://ao.osa.org/abstract.cfm?URI=ao-33-31-7547.
Woodard, R. P., M. G. Romania, and N. C. Tsamis, 2011, Classical and Quantum Gravity **28**(7), 075013.
Wu, L.-A., H. J. Kimble, J. L. Hall, and H. Wu, 1986, Phys. Rev. Lett. **57**, 2520, URL http://link.aps.org/doi/10.1103/PhysRevLett.57.2520.
Yagi, K., and T. Tanaka, 2010, Progress of Theoretical Physics **123**, 1069.
Yamamoto, H., 2007, personal communication.
Yamamoto, K., H. Hayakawa, A. Okada, T. Uchiyama, S. Miyoki, M. Ohashi, K. Kuroda, N. Kanda, D. Tatsumi, and Y. Tsunesada, 2008, Phys. Rev. D **78**, 022004.
Zucker, M. E., and S. E. Whitcomb, 1996, Proceedings of the Seventh Marcel Grossman Meeting on General Relativity .
ZygoEPO, 2011, ITM04 phasemap, Metrology Report.